Aging-associated Increase of GATA4 levels in Articular Cartilage is Linked to Impaired Regenerative Capacity of Chondrocytes and Osteoarthritis

Meagan J. Makarczyk[1,2,#], Yiqian Zhang[1,3,#], Alyssa Aguglia[2], Olivia Bartholomew[2], Sophie Hines[1,2], Suyash Sinkar[2], Silvia Liu[4,5], Craig Duvall[6], Hang Lin[1,2,7,*]

[1] Department of Orthopaedic Surgery, University of Pittsburgh School of Medicine, Pittsburgh, PA, USA

[2] Department of Bioengineering, University of Pittsburgh Swanson School of Engineering, Pittsburgh, PA, USA

[3] Xiangya Hospital, Central South University, Changsha, Hunan, China

[4] Department of Pharmacology and Chemical Biology, University of Pittsburgh School of Medicine, Pittsburgh, PA

[5] Organ Pathobiology and Therapeutics Institute, University of Pittsburgh School of Medicine, Pittsburgh, PA

[6] Department of Biomedical Engineering, Vanderbilt University, Nashville, TN, USA

[7] Bethel Family Musculoskeletal Research Center (BMRC), University of Pittsburgh School of Medicine, Pittsburgh, PA, USA

[#] These authors contributed equally

***Correspondence:**

Hang Lin, PhD

350 Technology Drive, Room 417, Pittsburgh, PA, 15219, USA

Phone: 412-624-5503; Fax: 412-624-5544

Email: hal46@pitt.edu

Abstract

Although the causal association between aging and osteoarthritis (OA) has been documented, our understanding of the underlying mechanism remains incomplete. To define the regulatory molecules governing chondrocyte aging, we performed transcriptomic analysis of young and old human chondrocytes from healthy donors. The data predicted that GATA binding protein 4 (GATA4) may play a key role in mediating the difference between young and old chondrocytes. Results from immunostaining and western blot showed significantly higher GATA4 levels in old human or mouse chondrocytes when compared to young cells. Moreover, overexpressing *GATA4* in young chondrocytes remarkably reduced their cartilage-forming capacity *in vitro* and induced the upregulation of proinflammatory cytokines. Conversely, suppressing *GATA4* expression in old chondrocytes, through either siRNA or a small-molecule inhibitor NSC140905, increased the production of aggrecan and collagen type II, and also decreased levels of matrix-degrading enzymes. In OA mice induced by surgical destabilization of the medial meniscus, intraarticular injection of lentiviral vectors carrying mouse *Gata4* resulted in a higher OA severity, synovial inflammation, and pain level when compared to control vectors. Mechanistically, we found that overexpressing GATA4 significantly increased the phosphorylation of SMAD1/5. Our work demonstrates that the aging-associated increase of GATA4 in chondrocytes plays a vital role in OA progression, which may also serve as a target to reduce osteoarthritis in the older population.

Keywords

GATA4, chondrocyte, aging, osteoarthritis, DNA damage

63 **Introduction**

64 Aging is an inevitable phenomenon resulting in limited functionality, loss of structural
65 integrity, and inability to effectively resist injury and disease.[1] Osteoarthritis (OA), the world's
66 most common form of degenerative disease, has been closely associated with the advancement of
67 age.[2] Specifically, OA is estimated to affect 32.5 million Americans, with most cases occurring in
68 adults over the age of 45.[3] In fact, 1 in 3 people over the age of 65 are suffering from OA.[4] There
69 are many contributors linked to the onset and progression of aging, such as organelle dysfunction
70 and telomere shortening,[1] but the molecular mechanism underlying age-related OA has not been
71 fully understood. Prior studies have demonstrated the role of DNA damage on chondrocyte aging
72 due to oxidative stresses, resulting in an aged phenotype. [5,6] Aged cells can also undergo a state
73 similar to permanent cell cycle arrest known as cellular senescence, which leads to a low-grade
74 state of chronic inflammation and contributes to OA onset and progression in aged individuals.[6-8]

75 OA is now considered a whole joint disease, but cartilage degradation still represents the
76 central feature.[3] The physiological role of articular cartilage is to support and protect the bones of
77 diarthrodial joints through absorbing mechanical loads and facilitating frictionless movements.
78 The extracellular matrix (ECM) of the cartilage is composed primarily of collagen type II and
79 glycosaminoglycans (GAGs), and the constant breakdown and rebuilding of ECM components in
80 the cartilage is common in healthy adults.[3,9] As we age, the regenerative response of chondrocytes
81 begins to decline.[2] The whole joint nature of OA and the limited regenerative capacity of
82 chondrocytes has contributed to the difficulty in developing disease-modifying osteoarthritis drugs
83 (DMOADs). To date, no DMOADs have reached FDA approval.[3]

84 Currently, OA-associated changes in chondrocytes have been widely examined, which
85 have significantly enhanced our understanding of this disease and promoted the development of
86 potential treatments. However, OA is a combined consequence of different physiological stressors,
87 including aging, injuries, obesity, etc. Therefore, aged chondrocytes in healthy humans without
88 OA do not necessarily exhibit all the features of OA chondrocytes. In this study, to understand key
89 regulators that contribute to an "aged" state in chondrocytes prior to OA onset, we first compared
90 the transcriptome of young and old human chondrocytes isolated from healthy donors without joint
91 diseases and employed unbiased analysis to define the key regulatory molecules that mediate
92 chondrocyte aging. Assessment of the chondrocyte genome demonstrated the upregulation of
93 several factors in aged chondrocytes, and transcription factor GATA binding protein 4 (GATA4)

specifically drew our attention since it is associated with DNA damage and cellular senescence.[5,10] Upregulation of GATA4 in OA chondrocytes was also reported.[11] We thus hypothesized that the increased GATA4 level contributes to chondrocyte aging and accelerated OA progression upon injuries. We first tested the hypothesis by increasing or suppressing *GATA4* expression in healthy chondrocytes and examining their cartilage-forming capacity. We also assessed the role of GATA4 *in vivo* by injecting lentiviral vectors carrying control or mouse *Gata4* genes into the knee joints of OA mice induced by surgically created destabilization of the medial meniscus (DMM). Lastly, a mechanistic study was conducted to explore how GATA4 impacts chondrocyte phenotypes and functions.

Materials and Methods

Cell isolation and expansion

Healthy human knee cartilage tissues were harvested from arthritis-free donors through an established protocol with the National Disease Research Interchange (NDRI). This study was approved by the University of Pittsburgh Committee for Oversight of Research and Clinical Training Involving Decedents. Cartilage was diced into ~ 1 mm^3 pieces with a scalpel and incubated with a dissociation medium that was composed of high glucose Dulbecco's Modified Eagle Medium (DMEM, Gibco/Thermo Fisher Scientific, Waltham, MA, United States), 2% Antibiotics-Antimycotics (Life Technologies, Carlsbad, CA, United States), and collagenase type II (1 mg/mL(w/v), Worthington Biochemical Corporation, Lakewood, NJ, United States). 10 mL medium was used for 1g of cartilage, and the treatment lasted for 16 hours in a shaker at 37°C. The mixture was then passed through a 70 μm strainer to collect single chondrocytes. Isolated chondrocytes were seeded in tissue culture flasks at 1×10^4 cells/cm^2 and maintained in growth medium (GM, DMEM containing 10% fetal bovine serum (FBS, Life Technologies) and 1% Antibiotics-Antimycotics). After cells were fully attached to the culture substrate, the medium was changed every three days until cells reached 70-80% confluency. Cells were detached with Trypsin/EDTA (Gibco/ Thermo Fisher Scientific) and passaged.

Individual Chondrocyte Monolayer Culture

Chondrocytes isolated from healthy human cartilage were expanded to passage 1 (P1) and plated in tissue culture 6 well plates at P2, treated with GM, and cultured until cells reached 80%

125 confluency. Media changes occurred every two days until cell collection. **Table S1** lists the
126 chondrocyte ages and genders used for different experiments.
127
128 **Young and Old Chondrocyte Pools**
129 Chondrocytes at passage 0 (P0) were pooled with three to four other young chondrocyte donors
130 and grown in tissue culture flasks with GM at a cell seeding density of $1x10^6$ cells per flask. Media
131 was changed weekly. Once cells reached 80% confluency, cells were collected using
132 Trypsin/EDTA. Some cells were frozen using Recovery Cell Culture Freezing Medium (Gibco/
133 Thermo Fisher Scientific), and other cells were used for subsequent passaging. The same methods
134 were used for the old (> 45 years) chondrocyte pool. **Table S1** lists the chondrocyte ages and
135 genders used in each pool. Due to the extensive amount of work conducted using these pools, two
136 separate chondrocyte pools were made.
137
138 **RNA sequencing (RNA-Seq) and bioinformatics analysis**
139 The transcriptomic differences among three young and three old chondrocyte donors were assessed
140 through RNA-Seq. Individual chondrocyte cultures (P0) were lysed with the QIAzol reagent
141 (Qiagen, German Town, MD, United States), and RNA was isolated from the lysate using an RNA
142 Easy Plus Universal Kit (Qiagen). Extracted RNA were quantitated Qubit™ RNA BR Assay Kit
143 (Thermo Fisher Scientific) followed by the RNA quality check using Fragment Analyzer (Agilent
144 Technologies, Santa Clara, CA). For each sample, RNA libraries were prepared from 500ng RNA
145 using the KAPA mRNA HyperPrep Kit (Roche, Indianapolis, IN) according to manufacturer's
146 protocol, followed by quality check using Fragment Analyzer (Agilent Technologies) and
147 fluorescent quantification on the Infinite F Nano + (Tecan, Männedorf, Switzerland). The libraries
148 were normalized and pooled, and then sequenced using NovaSeq6000 platform (Illumina, San
149 Diego, CA,) to an average of 50M 100PE reads.
150 Quality control was first applied to raw RNA sequencing reads by tool FastQC. Low-
151 quality reads and adapter sequences were filtered out by the Trimmomatic tool. Surviving reads
152 were then aligned to human reference genome hg38 using STAR aligner, and gene counts were
153 quantified. Differential expression analysis was performed based on gene counts by R package
154 "DESeq2" and DEGs were selected by adjusted p-value < = 0.05 and fold change > = 1.5. These
155 DEGs were then applied to Ingenuity Pathway Analysis (IPA) to detect enriched pathways. This

156 software employs databases of prebuilt pathways with known genes summarized from previous
157 studies, checks the overlap between the DEG list and known pathways and performs statistical
158 tests to determine the enrichment. Significant pathways were defined by p-value < = 0.05.
159 Statistically stringently, FDR = 5% cutoff should be applied to control the false discovery rate. To
160 encourage more gene candidates, this study went by p-value< = 0.05 and fold-change> = 1.5 cutoff.
161 All the tools were run by default parameter settings.
162
163 **Immunohistochemistry (IHC) to examine the GATA4 levels in native cartilage tissues.**
164 Human cartilage tissues were fixed in 10% buffered formalin (Fisher Chemical, Fair Lawn, NJ) at
165 4°C overnight and then subjected to a graded ethanol dehydration series, starting from 20% ethanol
166 and progressing to 100% ethanol. Subsequently, they were embedded in Paraplast X-tra (Leica
167 Biosystems Inc. Richmond, IL). The Paraplast-embedded samples were sectioned at a thickness
168 of 6 μm using a rotary Leica microtome (Leica Microsystems Inc., Deerfield, IL, Model RM 2255).
169 Young and old mouse knee joints were gifts from Dr. Ana Mario Cuervo's lab at Albert Einstein
170 College of Medicine, which otherwise were wastes. After the specimens were fixed and decalcified
171 in a formic acid-based bone decalcifier (StatLab, Mckinney, TX, USA) for a period of two weeks,
172 they were then embedded and sectioned as described above.
173 For immunohistochemistry (IHC), the formalin-fixed paraffin-embedded sections first
174 underwent antigen retrieval based on different antibodies. Slides were then blocked with 10% goat
175 or horse serum (Abcam, Cambridge, MA) in phosphate buffered saline (PBS, Thermo Fisher
176 Scientific) for 1h, incubated at 4°C overnight with the primary antibody against GATA4, then
177 incubated with a biotinylated anti-mouse/rabbit immunoglobulin G(IgG) secondary antibody for
178 1h, with signal detection via DAB substrate kit (Abcam). The Nikon Eclipse E800 upright
179 microscope (Melivile, NY, United States) was used to image the stained sections. Antibody
180 specifications can be found in **Table S2**.
181
182 **Western blot to examine the GATA4 levels in human chondrocytes**
183 P1 young and old chondrocytes were used for individual chondrocyte analysis of GATA4. Cells
184 were washed in pre-cooled PBS (Thermo Fisher Scientific) three times. Using the RIPA buffer
185 (Sigma-Aldrich) supplemented with the protease and phosphatase Inhibitor Single-Use Cocktail
186 (Gibco/Thermo Fisher Scientific) and a cell scraper, monolayer culture samples were collected. A

187 pestle was used to homogenize pellets in the RIPA cocktail for pellet culture samples. The protein
188 concentration of the supernatant was determined by the Pierce™ BCA Protein Assay Kit (Thermo
189 Scientific). Proteins were fractioned electrophoretically on the NuPAGE 4-12%, Bis-Tris Mini
190 Protein Gel (Gibco/Thermo Fisher Scientific) and then transferred to a polyvinylidene fluoride
191 (PVDF) membrane using the iBlot Dry Blotting System (Invitrogen, Waltham, MA, United States).
192 The membrane was blocked with 3% non-fat milk (Bio-Rad, Hercules, CA, USA), diluted with 1×
193 Tris-buffered saline (TBS, Gibco/ Thermo Fisher Scientific) and 0.1% Tween 20 (Sigma-Aldrich)
194 (TBST) at room temperature for 1.5 h, washed, and incubated with the primary antibody at 4°C
195 overnight on a rotating shaker. The membrane was washed 7 times for 3 min with TBST buffer
196 and incubated with horseradish peroxidase (HRP)-linked secondary antibodies (GE Healthcare
197 Life Sciences, Malborough, MA, United States) for 1.5 h at room temperature. After being washed
198 5 times with TBST, the membrane was incubated in the chemiluminescence substrate SuperSignal
199 West Dura Extended Duration Substrate (Thermo Fisher Scientific). Images were acquired using
200 the ChemiDocTM Touch Imaging System (Bio-Rad). Images were quantified using ImageJ.
201 Antibody information is included in **Table S2**.
202
203 **Overexpression of *GATA4* in young human chondrocytes**
204 P2 young, pooled chondrocytes or young, individual chondrocytes were transduced with the
205 lentiviral vector containing *GATA4* fused with dTomato gene or the control lentivirus carrying
206 EGFP for 10 hours. After that, flasks were rinsed with PBS for 2 times and the medium was
207 replaced by fresh GM. Both vectors were created and packed by VectorBuilder (>10^8 TU/mL,
208 VectorBuilder, Chicago, IL, United States). To detect the number of cells transduced, cultures were
209 imaged with an EVOS M5000 microscope (Thermo Fisher Scientific) after 72 h of initial
210 transduction. After transduction, western blot, RT-qPCR, and IHC were used to verify the stable
211 expression of GATA4 in cells.
212
213 **RNA isolation and quantitative real-time polymerase chain reaction (RT-qPCR)**
214 For pellet culture, samples were first rinsed with PBS twice and a pestle and electric pulverizer
215 were used to crush pellets. Cells were homogenized in Qiazol (Qiagen). Total RNA was isolated
216 and purified using the RNAeasy Plus Universal Mini Kit (Qiagen, Cat. NO. 74104) according to
217 the manufacturer's protocol. The reverse transcription to the complementary DNA (cDNA) was

218 accomplished using the SuperScript IV VILO Master Mix (Invitrogen). RT-qPCR was performed
219 on a real-time PCR instrument (QuantStudio 3, Applied Biosystems, Foster City, CA, United
220 States) using the SYBR Green Reaction Mix (Applied Biosystems) with custom primers ordered
221 from Integrated DNA Technologies (IDT, Newark, NJ, United States). Relative gene expression
222 levels were calculated through the $2^{-\Delta\Delta Ct}$ method. Ribosomal protein L13A (*RPL13A*) was used as
223 the housekeeping gene. Full names and abbreviations of genes and their corresponding proteins
224 are listed in **Table S3,** and primer sequences are listed in **Table S4**.
225
226 **Pellet culture and chondrogenesis of young human Chondrocytes overexpressing *GATA4***
227 Following the lentiviral transduction of *GATA4* gene in young, pooled chondrocytes, the cells were
228 collected and formed into pellets at a cell seeding density of 3×10^5 cells per pellet. Pellets were
229 treated with chondrogenic medium (CM, DMEM with 1% v/v Insulin-Transferrin-Selenium-
230 Ethanolamine (ITS, Gibco/ Thermo Fisher Scientific), 1% antibiotic-antimycotics, 10^{-7} M
231 dexamethasone (Sigma-Aldrich), 40 µg/mL L-proline (Sigma-Aldrich), supplemented with 10
232 ng/mL transforming growth factor- β3 (TGF- β3, Peprotech, Rocky Hill, NJ, United States), and
233 50 µg/mL ascorbic acid-2-phosphate (Sigma-Aldrich)). Medium was changed daily for seven days.
234 RT-qPCR, histology, IHC, and western blot were used to characterize the tissues.
235
236 **Safranin O/Fast green staining**
237 Pellet samples were fixed in 10% buffered formalin (Fisher Chemical) for 2 h at room temperature
238 and then rinsed with PBS. Pellets then underwent serial dehydration in 30,50,70,95, and 100%
239 ethanol for one hour each. The 100% ethanol was refreshed once for an additional hour prior to
240 sample clearing in Xylene. Pellets were cleared in Xylene (Fisher Chemical) for two hours. Pellets
241 were then placed in Paraplast X-tra (Leica Biosystems Inc.) overnight. The next day, pellets were
242 embedded in Paraplast X-tra blocks and sectioned at a 6-µm thickness using a Leica microtome
243 (Leica Microsystems Inc., Model RM 2255).
244 Slides were stained using Safranin O (0.5%, Catalog number: 50240, Sigma-Aldrich), in 1%
245 acetic acid (Catalog number: A6283, Sigma-Aldrich), 0.005% fast green (0.05 g, Catalog number:
246 104022, Sigma-Aldrich) in 100 mL distilled water (Invitrogen) and counterstained with
247 Hematoxylin QS solution (Catalog number: H3404, Vector Laboratories INC). Imaging was
248 conducted using a Nikon Eclipse E800 upright microscope.

249

250 **LUMINEX multiplex assays**

251 Upon 7 days of chondrogenesis, condition medium from pellets was collected and flash frozen in
252 liquid nitrogen and immediately stored in -80^{oC}. LUMINEX assays were accomplished using the
253 Bio-Plex 200 system (Bio-Rad). Data collection and analysis were conducted using the Bio-Plex
254 Manager 6.1 software as established in previous studies.[12] LUMINEX kit information can be found
255 in **Table S5**.

256

257 **Knockdown of *GATA4* in old human chondrocytes**

258 The siRNA targeting human *GATA4* (ON-TARGET plus Human GATA4 (2626) siRNA, J-008244-
259 06-0005, Horizon Discovery Biosciences Limited, Cambridge, UK) was used in this study with a
260 scrambled siRNA (ON-TARGET plus non-targeting siRNA #1, Catalog number: D-001810-01-
261 05, Horizon Discovery Biosciences Limited) as the control. Old, pooled chondrocytes were
262 transfected with the siRNA using Lipofectamine RNAiMAX reagent (Thermo Fisher Scientific).
263 After 24 hours of incubation, the transfection medium (Opti-MEM Reduced Serum Medium,
264 Thermo Fisher Scientific) was changed to GM. Transfected cells were collected after 48 hours for
265 RT-qPCR to confirm the knockdown efficiency.

266

267 **Pellet culture and chondrogenesis of old human chondrocytes with *GATA4* Knockdown**

268 Following the 48h transfection of scrambled control siRNA or siRNA targeting *GATA4* , cells were
269 collected using Trypsin/EDTA (Thermo Fisher Scientific) and pellets were made at a cell density
270 of $3x10^5$ cells per pellet. Pellets were treated with CM supplemented with 10 ng/mL TGF- β3 and
271 50 µg/mL ascorbic acid-2-phosphate for 7 days. Upon day 7, pellets were collected for RT-qPCR,
272 western blot, and IHC.

273

274 **GATA4 Small Molecule NSC140905**

275 GATA4 small molecule, NSC140905, also known as HCA 42027(Biosynth Ltd, Compton, United
276 Kingdom), was reconstituted to 7.5 mM stock solution using UltraPure™ DNase/RNase-Free
277 Distilled Water (Invitrogen) on a shaker at 37° until completely dissolved. Old, pooled
278 chondrocytes were pelleted and treated with CM supplemented with 10 ng/mL TGF- β3 and 50

279 μg/mL ascorbic acid-2-phosphate with 100 μM NSC140905 for 14 days. Pellets were collected for
280 IHC, western blot, and RT-qPCR.
281
282 **Animal model**
283 All animal experiments were approved by the University of Pittsburgh Institutional Animal Care
284 and Use Committee (IACUC). Young (8 weeks) male C57BL/6 mice were purchased from Jackson
285 Laboratory (Bar Harbor, ME, USA) and maintained in pathogen-free conditions, with no more
286 than five mice per cage. Mice were provided ad libitum access to food and water, and a 12-hour
287 light/dark cycle to simulate natural circadian rhythms. To minimize bias, mice were randomly
288 assigned to either control or GATA4 groups, with 8 mice in each group.
289
290 **Intraarticular injection**
291 Intraarticular injections were administered under general anesthesia to safeguard the well-being of
292 the animals and to minimize procedural discomfort. Under general anesthesia with 2% isoflurane
293 in an oxygen mixture, the mice were placed in a supine position, and the right knee joint was
294 positioned at a 90-degree flexion to facilitate accurate injection into the joint space. The injection
295 site was meticulously identified medial to the patellar tendon. Using a 29-gauge needle, a volume
296 of 10 μL of lentiviral particles encoding either GATA4 or a control vector (at a concentration $>10^8$
297 TU/mL, VectorBuilder) was precisely administered into the intra-articular space of the right knee.
298 The precision of the injection was ensured by employing a consistent technique across all animals,
299 thereby reducing variability in the delivery of the viral vectors.
300
301 **Destabilization of the medial meniscus (DMM) surgery**
302 One week after viral vector injection, DMM surgery was performed to induce the OA model.[13,14]
303 Briefly, a medial parapatellar incision was made to expose the right knee joint, followed by a
304 careful opening of the joint capsule. The anterior medial menisco-tibial ligament was identified
305 and transected using micro scissors. The joint capsule and skin were subsequently sutured with 6-
306 0 silk thread. For experimental controls, a sham operation was performed in which the joint capsule
307 was exposed as in the DMM surgery, but the medial menisco-tibial ligament was left intact.
308
309 **Knee hyperalgesia**

310 We expected accelerated OA development after *Gata4* overexpression. To observe these
311 differences, we used six weeks as the time point at which control mice had begun displaying mild
312 OA symptoms. Knee hyperalgesia was evaluated using a Pressure Application Measurement
313 (PAM) device (Ugo Basile, Varese, Italy).[15,16] Mechanical stimuli were applied to the mouse's knee
314 joint to assess the degree of hyperalgesia based on the applied pressure and the mouse's response.
315 Six weeks after either DMM or sham surgery, the mice were carefully removed from their cages
316 to ensure they remained calm and unstimulated. The mouse was held securely by its back to
317 maintain a straight posture, with the right knee joint flexed at approximately 90 degrees. The PAM
318 device was placed on the index finger of the right hand of testers, which, along with the thumb,
319 was used to apply pressure to the medial side of the knee joint, ensuring proper contact. Pressure
320 was gradually applied at a constant rate of 30 g/s while monitoring the pressure curve displayed
321 on the computer. The sensor was released immediately when the mouse exhibited a response to
322 the applied stress, such as head movement, vocalization, or knee withdrawal. The pressure value
323 displayed by the software, and the maximum pressures that mice can withstand were recorded.
324 Two measurements were taken per knee, one on the medial side, and one on the lateral side the
325 average was calculated for accuracy.
326
327 **Synovial inflammation score**
328 After 6 weeks, knee joints were collected and sectioned as described above. Histology staining
329 and IHC were used to assess OA severity. Synovial inflammation score was evaluated according
330 to a scoring protocol outlined in previous studies[17], which relies on the hematoxylin and eosin
331 (H&E)-stained tissue sections.
332
333 **Statistical Analysis**
334 Each experiment was carried out with at least three biological replicates. Data is presented as mean
335 ± standard deviation unless otherwise specified. Detailed information of sample size, pre-
336 processing, and statistical methods have been specified in each figure legend. Prism 10 (GraphPad,
337 San Diego, CA) was used for statistical analysis. The significance level was set at 0.05 and
338 indicated by * ($p < 0.05$), ** ($p < 0.01$), *** ($p < 0.001$), and **** ($p < 0.0001$).
339

340 **Results**

341 *GATA4 is predicted to regulate chondrocyte aging*

342 To limit the influence of *in vitro* expansion on cell phenotype, P0 human chondrocytes
343 were used for RNA sequencing (**Figure 1A**). The volcano plot showed that 303 genes are
344 upregulated and 163 genes are downregulated in aged chondrocytes compared to young cells
345 (**Figure 1B**). The top 50 most changed genes are listed in **Figure 1C**. Interestingly, the
346 osteoarthritis pathway was identified to be activated in old chondrocytes (**Figure 1E**).

347 Through Ingenuity Pathway Analysis (IPA) Upstream Regulator Analysis, transcriptional
348 regulators that may mediate the difference between young and old cells were predicted, and the
349 top 20 of them are shown in **Figure 1D**. Given that GATA4 was previously shown to regulate
350 chondrocyte senescence[10] and be involved in the activation of Nuclear Factor Kappa B (NF-κB)
351 pathway in tissues like the nucleus pulposus[18] and synovium,[19,20] it was selected for further
352 investigation in this study. Initial data analysis predicted that GATA4 was upregulated in aged
353 chondrocytes compared to young donors (**Figure 1D**). Immunohistochemistry (IHC) results
354 indicated that GATA4 was more abundant in articular cartilage harvested from aged individuals
355 (**Figure 1F**) (**Supplementary Figure S1**). Analyzing knee joints collected from young and old
356 mice also demonstrated that GATA4 levels were higher in aged cartilage tissues compared to young
357 (**Supplementary Figure S2**). To further confirm the findings, western blot was used to examine
358 GATA4 levels in isolated chondrocytes, and the results indicated that aging correlates with the
359 increase of GATA4 in chondrocytes (**Figure 1G**).

360

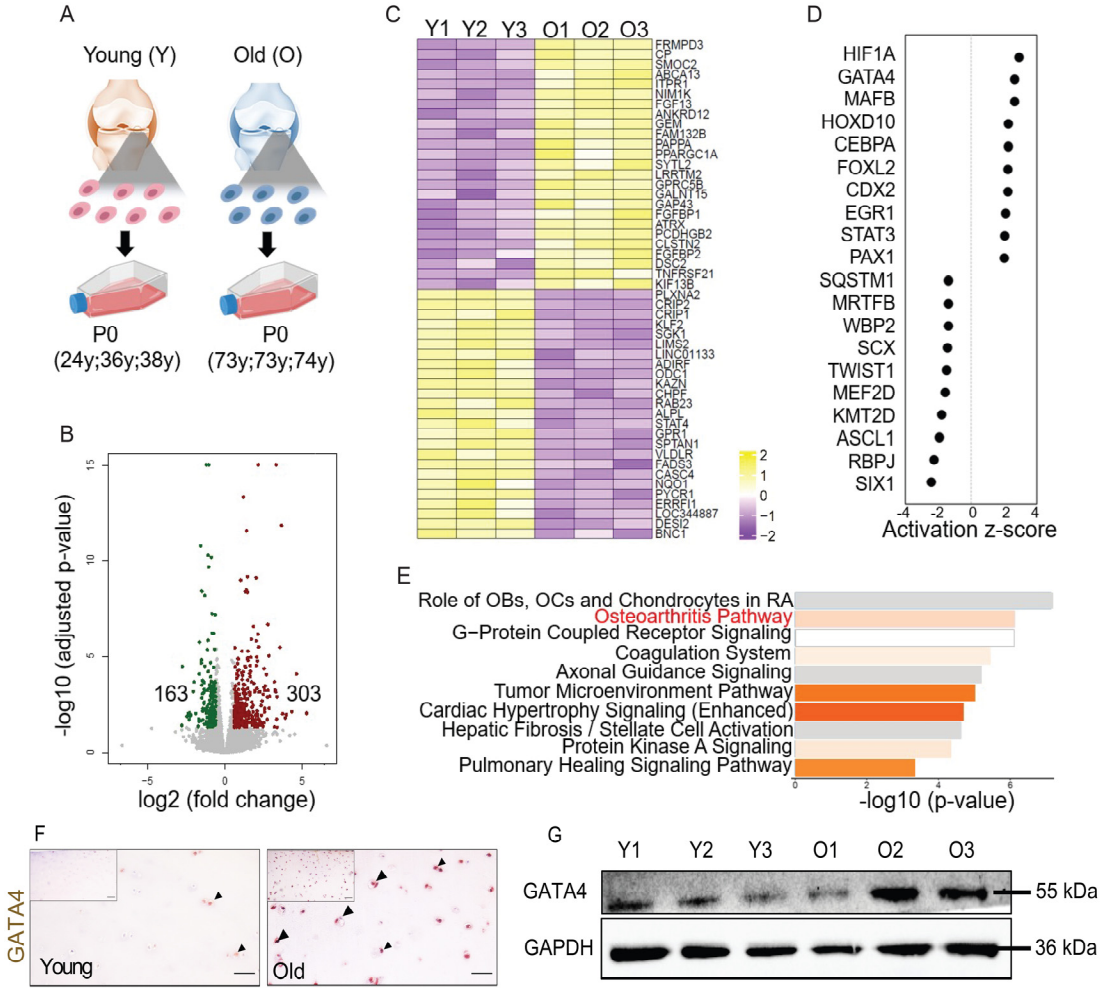

Figure 1*: Bulk RNA sequencing to compare the transcriptome differences between young and old chondrocytes.** *(A) Healthy chondrocytes were isolated from knee joint cartilage from young and old donors without osteoarthritis (assessed by experienced surgeons). P0 cells were used for RNA sequencing analysis. (B) Volcano plot demonstrating 303 upregulated and 163 downregulated genes in old chondrocytes when compared to young cells. (C) Top 50 genes that are significantly differently expressed in young and old chondrocytes. (D) Activation Z score of top 10 transcription regulators that are activated (positive) or inhibited (negative) in aged versus young chondrocytes. A comprehensive list of gene names can be found in* ***Table S3*. (E) Ingenuity Pathway Analysis (IPA) of young versus old cells. The gray bars indicate that no activity pattern is identified in IPA despite the highly significant association of the genes within the pathway. Orange, positive z-score; white, zero z-score. OBs=osteoblasts; OCs=osteoclasts. (F) GATA4 IHC of healthy human cartilage tissue from young and aged donors. Bar=50 µm. (G) Relative protein levels of GATA4 in P1 chondrocytes from individual human donors were analyzed by western blot.*

375

376 *Overexpressing GATA4 impairs the hyaline cartilage formation capacity of young chondrocytes*

377 To examine the functions of GATA4 in chondrocytes, we first overexpressed it in healthy
378 young human chondrocytes (**Figure 2A**). Real-time quantitative PCR (RT-qPCR),
379 immunostaining, and western blot confirmed the significantly increased GATA4 expression after
380 infection, which did not impact the expression levels of collagen type II (COLII)-α1 (*COL2A1*)
381 and aggrecan (*ACAN*), but significantly upregulated the expression of Collagen type X (COLX)-
382 α1 (*COL10A1*) and India hedgehog (IHH), two representative chondrocytic hypertrophy markers
383 (**Supplementary Figure S3**). We then examined the cartilage formation capacity of cells by
384 culturing cells in chondrogenic medium for 7 days. IHC, RT-qPCR, and western blot demonstrated
385 the continuous overexpression of *GATA4* in newly formed tissues (**Figure 2B-D**). Interestingly,
386 significantly reduced GAG and COLII production was found in the overexpression *GATA4* group
387 (GATA4 group) compared to the GFP control group (**Figure 2E-G**). Similar results were observed
388 in the study testing chondrocytes from individual donors (**Supplementary Figure S4**).
389 Interestingly, *GATA4* overexpression did not impact the expression of *COL10A1* and *IHH* in the
390 cartilage pellets **(Figure 2G**). Additionally, tissues from the GATA4 group secreted more
391 proinflammatory cytokines, including IL-6, IL-8, TNF-α, and chemokine CCL2 (**Figure 2H&I**),
392 as well as enzymes that can break down cartilage, including matrix metalloproteinases *(MMP)-1,*
393 *2, 12*, and a disintegrin and metalloproteinases *(ADAMTS) 5* (**Figure 2J&K**). Although the
394 expression levels of *MMP-13* gene decreased in GATA4 group, the protein levels showed no
395 difference between the two groups (**Supplementary Figure S5**).

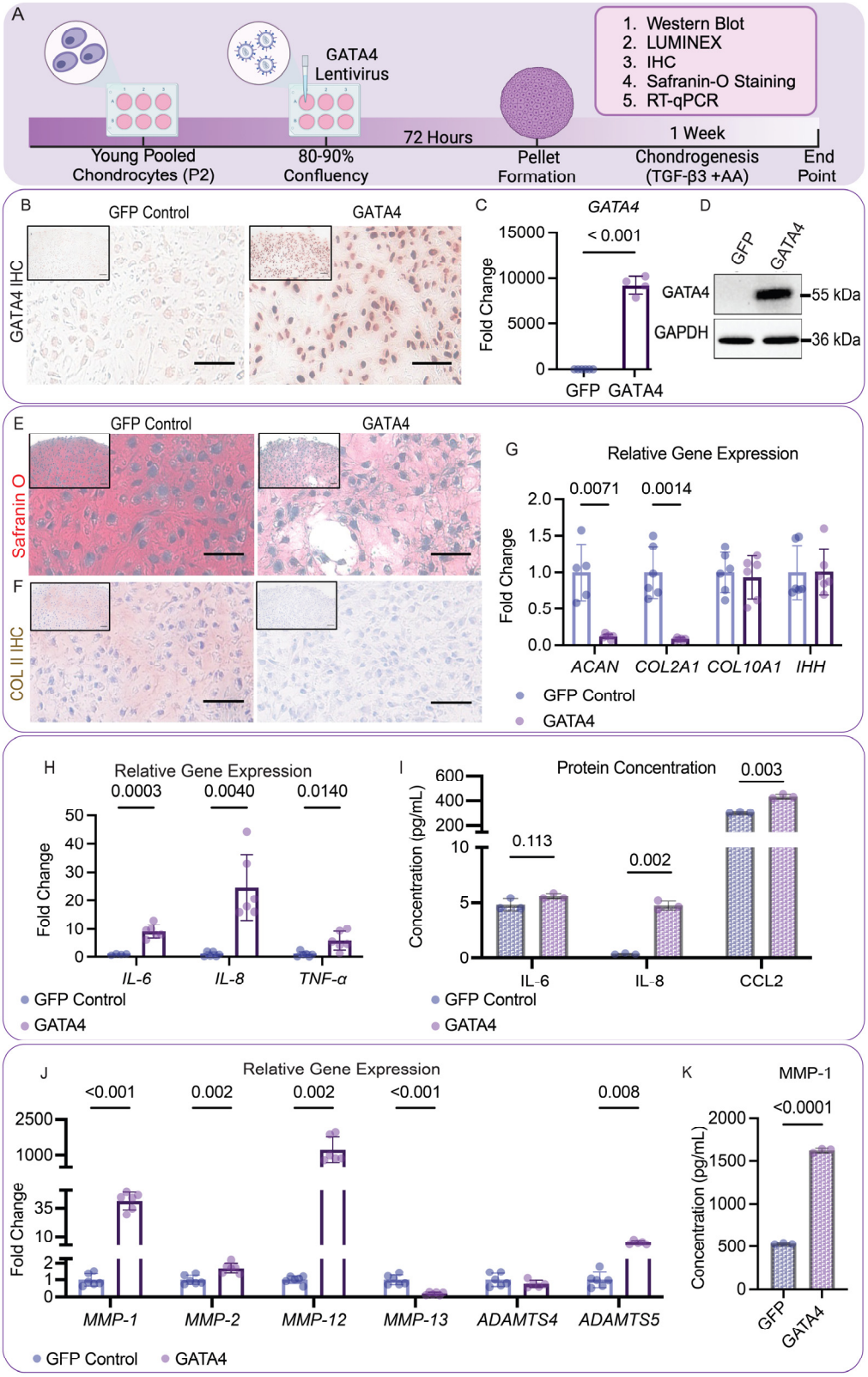

***Figure 2**: **Impact of GATA4 overexpression on in vitro cartilage formation of young chondrocytes.** (A) Timeline depicting the study. (B) IHC to assess GATA4 protein levels in young*

399 *cells overexpressing GFP control or GATA4. Scale Bar=50 µm. (C) RT-qPCR analysis of GATA4*
400 *gene expression in two groups. (D) Western blot to measure GATA4 protein levels. (E) Safranin O*
401 *staining and (F) Collagen type II (COLII) IHC to examine the production of cartilage matrix.*
402 *Scale Bar=50 µm. (G) RT-qPCR analysis of gene expression of cartilage matrix proteins aggrecan*
403 *(ACAN) and collagen type II-α1 (COL2A1) and hypertrophy markers collagen type X- α1*
404 *(COL10A1) and India hedgehog (IHH). (H) RT-qPCR analysis of gene expression of*
405 *proinflammatory cytokines, including interleukin (IL)-6, IL-8, and tumor necrosis factor- α* (*TNF-*
406 *α*) (n=6). *(I) Concentrations of IL-6, IL-8, and chemokine (C-C motif) ligand 2 (CCL2) in condition*
407 *medium* (n=3). (*J) RT-qPCR analysis of relative gene expression of matrix-degrading enzymes,*
408 *including matrix metalloproteinases (MMP)-1,2,3,12, and 13, and a disintegrin and*
409 *metalloproteinase (ADAMTS) 4 and 5* (n=6). *(K) MMP-1 concentration in condition medium*
410 (n=3). *Student's two-tailed t-test with Welch's correction for standard deviation and a p-value of*
411 *0.05 was used for all statistical analysis.*
412
413
414 *GATA4 overexpression activates SMAD1/5*
415 Increased SMAD1/5 phosphorylation represents a key feature of aged chondrocytes [21]. We
416 thus examined whether increased GATA4 levels are associated with SMAD1/5 activation (**Figure**
417 **3A**). In the experiment testing chondrocytes from individual donors (**Figure 3B, D-G**),
418 overexpression of GATA4, even without the stimulation of TGF-β3, was sufficient to activate
419 SMAD1/5, but not SMAD2/3. In addition, the group that was co-treated with GATA4
420 overexpression and TGF-β3 displayed the highest phosphorylated SMAD1/5 (pSMAD1/5) levels
421 in all tested groups. Of note, activation of SMAD2/3 was not impacted by GATA levels. A similar
422 trend was also observed in the study using pooled chondrocytes (**Figure 3C**).
423

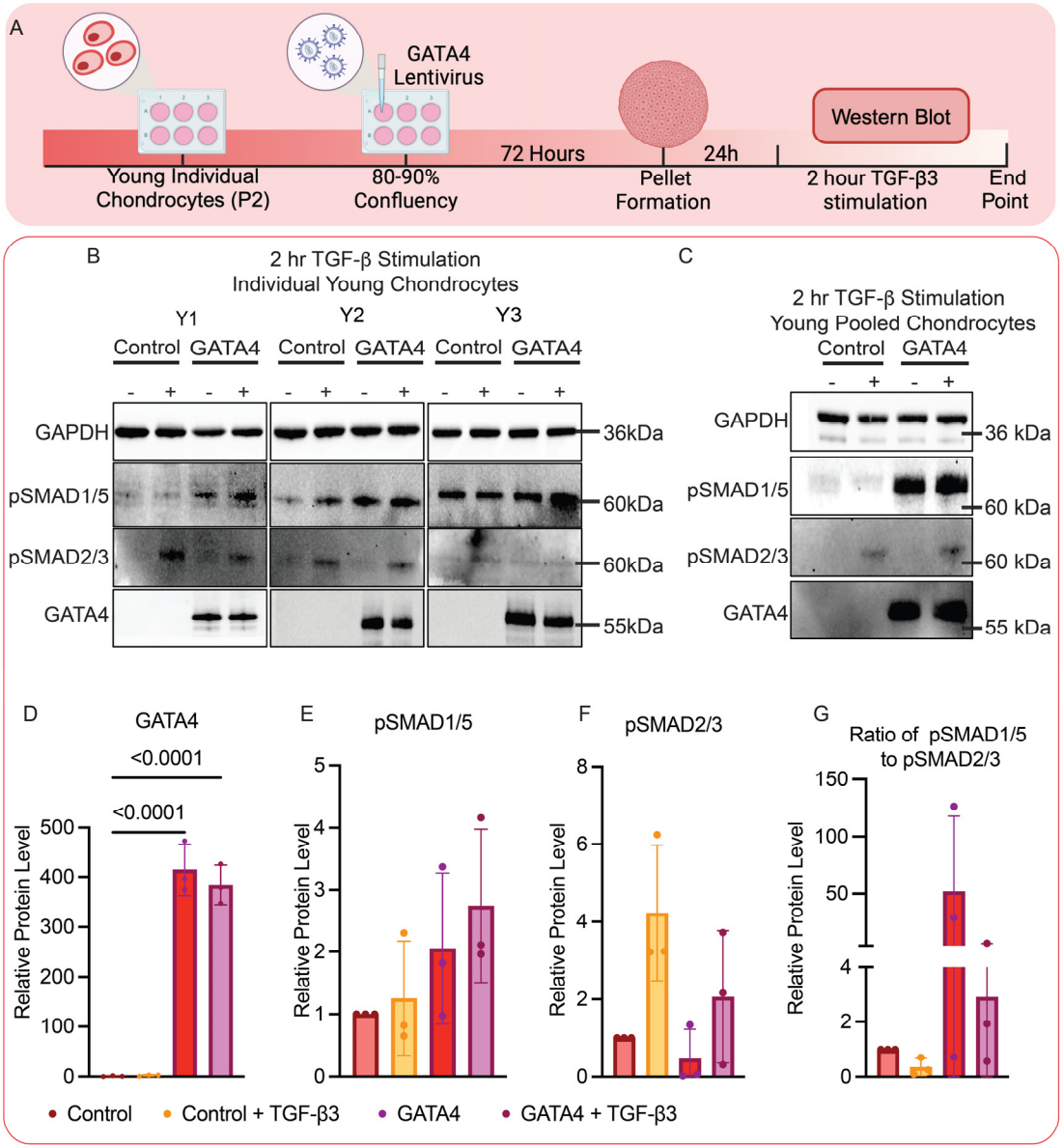

Figure 3: Assessment of activation of SMADs following GATA4 overexpression. *(A) Schematic showing the experiment. (B, C) Western blot to assess protein levels of phosphorylated SMAD1/5 (pSMAD1/5), phosphorylated SMAD2/3 (pSMAD2/3), and GATA4 in pellets derived from young (B)individual(Y1-3) or (C) pooled chondrocytes, which were infected with lentiviral vectors carrying GATA4 or control genes and then stimulated with (+) or without (-) TGF- β3 for two hours. Relative protein levels of (D)GATA4, (E)pSMAD1/5, and (F)pSMAD2/3 were semi-quantified using ImageJ (n=3). (G) The ratio of pSMAD1/5 compared to pSMAD2/3 was also calculated. Statistics were conducted using one-way Analysis of Variance (ANOVA) with Dunnett's post hoc analysis.*

434 *Suppressing GATA4 in old chondrocytes promotes ECM formation and lowers proinflammatory*
435 *cytokines*

436 We then tested the potential of suppressing GATA4 in reversing chondrocyte aging (**Figure**
437 **4A**). Several GATA4 siRNAs were tested, and the one with the highest efficiency was selected
438 (**Supplementary Figure S6**). *GATA4* knockdown resulted in increased cartilage formation from
439 old chondrocytes, which did not influence the expression of hypertrophy marker *COL10A1*
440 (**Figure 4B-D**). Moreover, although we did not see a difference between scrambled control and
441 GATA4 siRNA groups regarding the expression of *IL-6* and *IL-8*, the protein level of IL-8 was
442 higher in the GATA4 group. Interestingly, the protein level of CCL2 was significantly decreased
443 after GATA4 knockdown (**Figure 4E, F**). We also tested the expression levels of MMPs and
444 ADAMTSs (**Figure 4H-I**). In general, suppressing GATA4 either decreased or caused no
445 significant changes to the levels of these enzymes. In particular, MMP-13 levels were reduced, in
446 both gene and protein levels (in condition medium), after GATA4 knockdown. Mechanistically,
447 GATA4 siRNA treatment also lowered the phosphorylation of SMAD1/5 and p-P65 (**Figure 4G**).

448 In a separate study, we used a small-molecule GATA4 inhibitor NSC140905, which was
449 shown to significantly promote cartilage formation from old chondrocytes and reduce the
450 expression of proinflammatory cytokines (**Supplementary Figure S7**). Taken together,
451 suppressing GATA4 partially restored the capacity of old chondrocytes to create new cartilage.
452

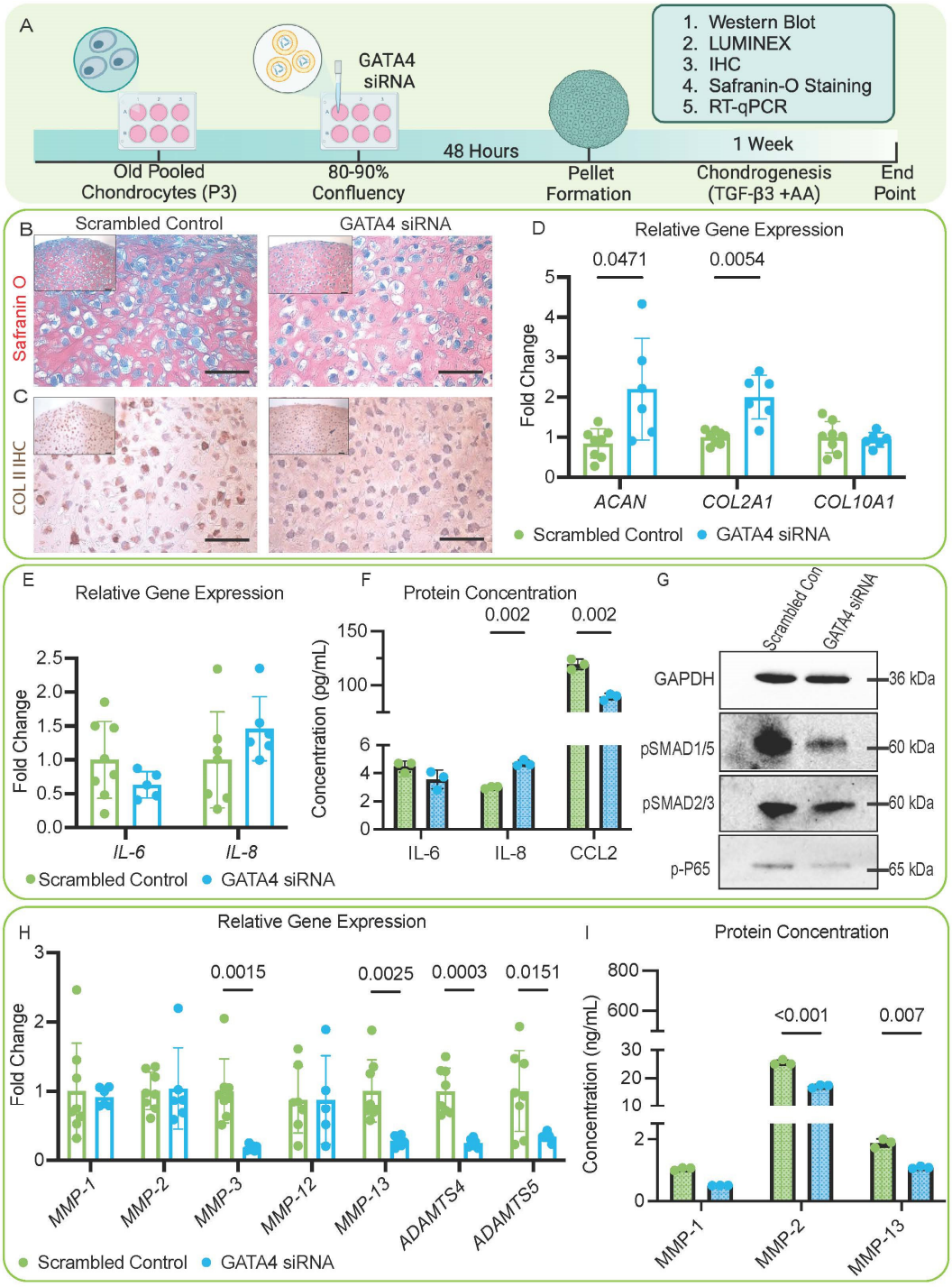

Figure 4: Influence of GATA4 knockdown on in vitro cartilage formation of old chondrocytes. *(A) Schematic showing the study. (B) Safranin O staining and (C) COLII IHC to examine the production of cartilage matrix in the Scrambled Control or GATA4 siRNA group. Scale Bar=50 µm. (D) RT-qPCR analysis of relative gene expression of cartilage matrix proteins ACAN and COL2A1 and hypertrophy marker COL10A1*(n=6). *(E) RT-qPCR analysis of relative gene*

expression of proinflammatory cytokines IL-6 and IL-8 (n=6). (*F*) *Concentrations of IL-6, IL-8, and chemokine (CCL2) in condition medium* (n=3). (*G) The relative protein levels of pSMAD1/5, pSMAD2/3, and phosphorylated p65 (p-P65) in two groups. (H) RT-qPCR analysis of relative gene expression of matrix-degrading enzymes, including MMP-1,2,3,12, and 13, and ADAMTS 4 and 5* (n=6). *(I) MMP-1,2 and 13 concentrations in condition medium* (n=3). *Student's two-tailed t-test with Welch's correction for standard deviation and a p-value of 0.05 was used for all statistical analysis.*

Gata4 overexpression in the knee joints accelerates OA progression in mice

The physiological functions of GATA4 were further examined using a mouse model (**Figure 5A**). Specifically, lentiviral vectors carrying *Gata4* or *mCherry* genes were injected into the knee joints of young mice. One week after the injection, DMM surgery was conducted to induce OA. Since we expected that Gata4 overexpression would accelerate OA progression, we harvested samples for analysis 6 weeks after DMM.

Results from IHC indicated a successful Gata4 overexpression in hyaline cartilage even 6 weeks after injection (**Figure 5B, C**). Interestingly, mice overexpressing Gata4 in the knee joint resulted in the elevation of p-P65 (**Figure 5D, E**), suggesting increased inflammation. Moreover, the mice in the Gata4 group displayed a more severe OA and higher knee hyperalgesia than the control group, revealed by a lower withdrawal threshold (**Figure 5F-H**). Interestingly, mice from the Gata4 group displayed higher synovial inflammation (**Figure S8**).

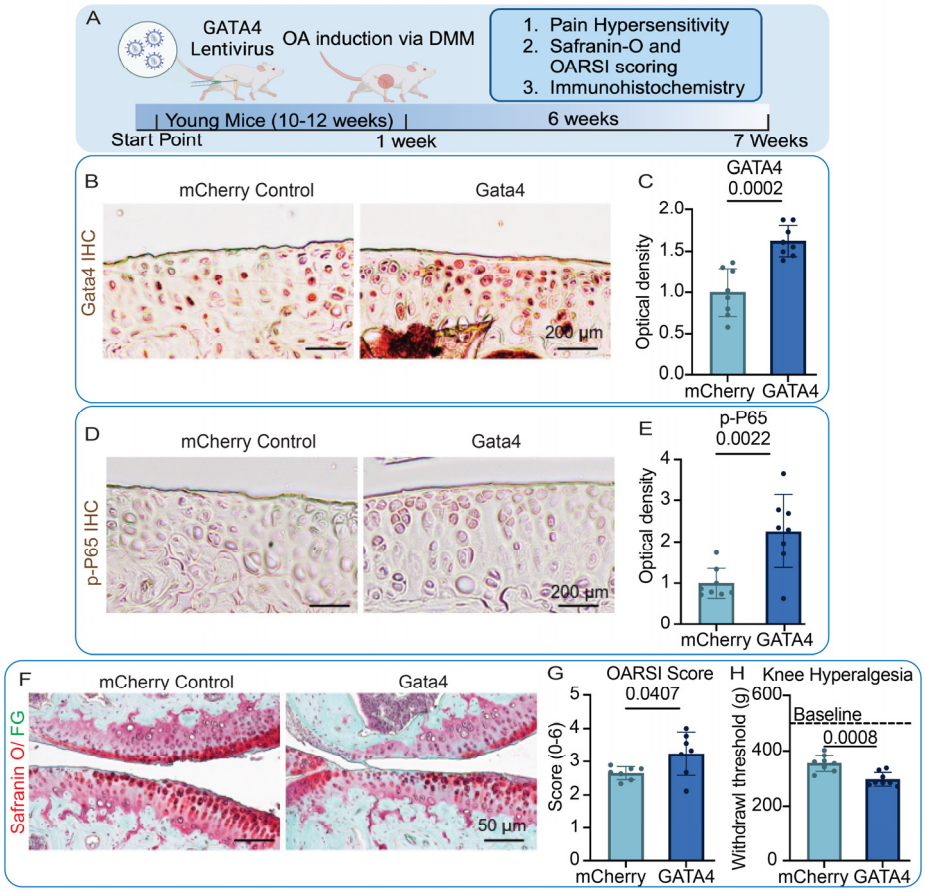

Figure 5: Assessment of the physiological roles of Gata4 through intraarticular overexpression. *(A) schematic of the study. Mice received one intraarticular injection of lentiviral vectors that carried mCherry or Gata4 gene one week before DMM surgery was performed. Knee joints were harvested 6 weeks post-surgery. Levels of Gata4 (B, C) and p-P65 (D, E) were assessed with IHC(B&D), and the staining was semi-quantitated with Image J (C&E). Cartilage degradation was assessed with (F) Safranin O/ fast green (FG) staining, and (G)OARSI score was calculated. (H)Knee hyperalgesia 6 weeks post-surgery. 507 g was the threshold baseline for non-surgery mice (dashed line). Student's two-tailed t-test with Welch's correction for standard deviation and a p-value of 0.05 was used for all statistical analysis.*

Discussion

The causal relationship between aging and OA has been documented, and understanding the molecular mechanisms is essential for the development of treatment methods. In this study, we discovered the critical roles of aging-associated increases in GATA4 levels. Specifically, overexpressing GATA4 in young chondrocytes impaired their capacity to form normal hyaline

496 cartilage, while suppressing GATA4 in old chondrocytes restored their chondrogenic potential. We
497 also demonstrated that GATA4 functions partially by promoting the activation of SMAD1/5. Our
498 *in vivo* work further confirmed that high *Gata4* expression accelerated OA progression in mice.
499 Lastly, we defined a small-molecule GATA4 inhibitor that can partially restore the capacity of old
500 chondrocytes to create healthy cartilage, representing a potential DMOAD for further validation
501 in the future.

502 Given the recognized challenges in harvesting healthy cartilage tissues from donors without
503 arthritis, there are limited reports investigating chondrocyte aging per se. The current findings
504 include proliferation and post-expansion chondrogenic capacity reduction with aging,[22] increased
505 MMP-13 production in response to catabolic stimuli,[23] and altered response to TGF-β.[24] One of
506 our recent studies again demonstrated that aged chondrocytes displayed a reduced proliferation
507 potential compared to young cells. Additionally, cartilage tissues generated by old chondrocytes
508 contained more senescent cells than those from young cells.[25] However, to the best of our
509 knowledge, there were no publications describing the transcriptomic comparisons between young
510 and old chondrocytes, which would be informative in defining targets to stop or reverse
511 chondrocyte aging.

512 Through transcriptomic analysis, we were able to assess the expression of different genes and
513 genetic pathways that occur as chondrocytes age and found that GATA4 was predicted to have a
514 higher z score in aged chondrocytes. The GATA family consists of several proteins (GATA1-6)
515 with different variations of DNA-binding domains composed of zinc finger structures.[18]
516 Particularly, GATA4, 5, and 6 are involved in the development of the mesoderm and endoderm
517 tissues,[26] in which GATA4 has been detected in the development of structures such as the heart,[27,28]
518 pancreas,[29] lung, and liver.[30,31] In addition, GATA4 and GATA6 are the only members that are
519 associated with aging.[32] Particularly, GATA4 is unique in that it regulates tissues in a context-
520 dependent manner and adopts a multifaceted role in the body, contributing to other age-related
521 diseases such as atherosclerosis[33] and heart failure.[34]

522 In 2015, GATA4 was first introduced as a senescence regulator in a study conducted by
523 Kang et al.[10] This work demonstrated the role of GATA4 in human fibroblasts and determined that
524 the inhibition of autophagy caused GATA4 accumulation following DNA damage. They examined
525 the presence of GATA4 in the human brain and found that there was an increase of GATA4 in the
526 prefrontal cortex of aged human samples.[10] In fact, previous studies demonstrated that increased

527 GATA4 levels are associated with chondrocyte senescence,[11,35,36] an important change often
528 observed in OA chondrocytes. Moreover, suppressing GATA4 with siRNA was shown to
529 effectively abolish ionizing radiation-induced senescent phenotype in chondrocytes.[11] Of note, all
530 these studies relevant to chondrocytes were conducted *in vitro*. Herein, we, for the first time,
531 demonstrate the role of GATA4 in regulating chondrocyte aging.

532 A theory of chondrocyte aging proposed by van der Kramm suggests that alterations to the
533 TGF-β pathway induce chondrocyte hypertrophy and result in articular cartilage that is prone to
534 OA development.[24] While investigating the function of GATA4 in chondrocytes, we assessed how
535 its levels contribute to TGF-β alterations in chondrocytes and found that GATA4 levels negatively
536 correlated with the anabolic potential of chondrocytes (**Figures 2 and 4**). To maintain healthy
537 cartilage homeostasis, numerous pathways are involved. In particular, TGF-β is a crucial cytokine
538 involved in cartilage homeostasis during OA,[37,38] and aged chondrocytes respond differently to
539 TGF-β compared to their young counterparts.[39] Mechanistically, in the TGF-β pathway, TGF-β
540 binds to the heterotetrameric receptor complex, which can be grouped into three receptor types
541 (type I, type II, and type III). When TGF-β binds to its corresponding receptor, the activin-receptor-
542 like kinases (ALKs) are activated.[40] Typically, the anabolic binding of TGF-β to ALK4/5 results
543 in the phosphorylation of SMAD2/3, protecting chondrocytes from hypertrophy.[37] However, there
544 can also be catabolic effects associated with the expression of SMAD1/5, typically expressed when
545 TGF-β binds to ALK1/2/3/6.[37,40] The phosphorylation of SMAD1/5 results in the promotion of
546 ECM degrading proteins such MMP13.[21,37] As mentioned previously, research has demonstrated
547 that aged chondrocytes respond differently to TGF-β compared to young chondrocytes.[39,41]
548 Chondrocyte aging has been linked to the increase of pSMAD1/5 signaling.[21] These previous
549 studies inspired us to explore the potential association between GATA4 levels and the activation
550 of SMAD1/5. Our results found that GATA4 resulted in the phosphorylation of SMAD1/5 even
551 without TGF-β stimulation, which however did not alter the phosphorylation of SMAD2/3.
552 Although there are no current publications specifying the complex relationship of GATA4 and
553 SMAD1/5 in chondrocytes, a prior study reported that GATA4 was regulated by SMAD1/5.
554 Specifically, they can bind together to promote IL-6 expression in macrophages.[42]

555 While TGF-β pathway is closely associated with cartilage matrix remodeling, we also found
556 increases in the levels of multiple proinflammatory cytokines after GATA4 overexpression. We
557 investigated the NF-κB pathway since it is also activated during aging. [43,44] During the aging

558 process, NF-κB is thought to amplify and potentially propagate cellular senescence through the
559 senescence-associated secretory phenotype (SASP).[45] A study by Qiao et al. indicated that GATA4
560 regulates NF-κB in dental pulp cells[46] and fibroblasts[47]. Specifically, using siRNAs, they
561 determined that the knockdown of GATA4 decreased p65 production induced by
562 lipopolysaccharide (LPS).[46] Other studies have investigated the role of GATA4 in the synovium
563 and the progression of the disease state of rheumatoid arthritis and OA. Jia et al. showed that the
564 knockdown of GATA4 attenuated synovial inflammation and joint damage in a collagenase-
565 induced arthritis mouse model.[47] More recently, a study conducted by Chen et al. investigated the
566 roles of GATA4 in fibroblast-like synoviocytes (FLS) and determined that GATA4 induced cellular
567 senescence in FLSs and their role in OA progression.[20] Our study also discovered that the siRNA
568 knockdown of GATA4 decreased the phosphorylation of p65 in aged chondrocytes (**Figure 4**).
569 However, we also noticed that MMP-13 expression levels decreased in both *GATA4*
570 overexpression and knockdown experiments. It should be noted that MMP-13 is constitutively
571 produced in human chondrocytes but is only activated under pathological conditions. Given that
572 MMP-13 is regulated by different transcriptional factors and cytokines, as well as RNAs,[21] its
573 associations with GATA4 require further investigation in the future. Collectively, these findings
574 further indicate that GATA4 might regulate aging partially through TGFβ and NF-κB pathways.
575 Our current study has not fully explored why aging promotes GATA4 expression. The study
576 from Kang et al. indicated that DNA damage contributed to GATA4 accumulation.[10] It is known
577 that DNA damage response (DDR) is regulated by ataxia telangiectasia mutated (ATM) and ataxia
578 telangiectasia and Rad3–related (ATR) signaling.[10,48,49] The activation of these signaling pathways
579 inhibits autophagy-related protein p62.[50] In addition, Copp et al. reported increased DNA damage
580 in old chondrocytes.[5] These studies implied that DNA damage may be a reason for GATA4
581 upregulation. Our preliminary data support this possibility. Specifically, a DNA damage-inducing
582 agent, doxorubicin, promoted the upregulation of GATA4 in chondrocytes (**Supplementary**
583 **Figure S9**). To further link DNA damage to GATA4 accumulation, a study by Chung et al. used
584 Tributyltin (TBT), a well-known endocrine-disrupting chemical, to induce DNA damage in
585 articular chondrocytes. After 24 hours of TBT treatment, there was a significant increase in *GATA4*
586 expression and expression of senescence markers.[35] Therefore, we believe that DNA damage due
587 to aging is a key driver of the upregulation of GATA4 in old chondrocytes.

588 In conclusion, we have determined that GATA4 is increased in aged chondrocytes compared
589 to young in both humans and mice, which may be induced by increased DNA damage observed in
590 aged cells. We also demonstrated that GATA4 overexpression impaired the quality and quantity of
591 cartilage created by chondrocytes and accelerated OA progression in mice. Conversely,
592 suppressing GATA4 with siRNA or small-molecule inhibitors partially restores the capacity of old
593 chondrocytes to form cartilage. Additionally, our study found that GATA4 can activate SMAD1/5
594 and change chondrocyte response to TGF-β. Overall, our study indicated that GATA4 could be a
595 contributor to OA onset and progression in aged individuals, which can also serve as a potential
596 target to prevent aging-associated OA.
597 There are some limitations of this study that can be further addressed in future studies. First,
598 this study has allowed us to examine the potential mechanisms of GATA4 in chondrocyte aging.
599 However, the relationship between GATA4 overexpression and SAMD1/5 activation should be
600 further investigated to elucidate specific signaling mechanisms. Second, during our *in vivo* work,
601 the intraarticular injection of GATA4 lentivirus was not tissue-specific. Therefore, the injection
602 allowed for other cell types to overexpress GATA4. Future work should be conducted with
603 cartilage-specific overexpression or depletion of GATA4 to clarify findings. Furthermore, studies
604 using GATA4 knockdown do not demonstrate a complete reversal of aging in chondrocytes, and
605 additional *in vivo* assessment needs to be conducted to verify whether GATA4 could be a
606 therapeutic target for chondrocyte aging, in particular, the potential use of small molecule GATA4
607 inhibitor studied here. Lastly, our work indicates that GATA4 has a role in chondrocyte aging, but
608 that does not negate the other aging factors and pathways. Combining current findings and
609 investigating the prevalence of GATA4 in association with other aging molecules will further
610 contribute to our understanding of the role of GATA4 in aging and possible OA onset.
611
612 **Acknowledgments**
613 This work was supported by the Department of Orthopaedic Surgery and the Orland Bethel Family
614 Musculoskeletal Research Center (BMRC) at the University of Pittsburgh, as well as the
615 University of Pittsburgh Center for Research Computing through the resources provided. This
616 study used the Luminex Core Facility of UPCI. M.J.M was supported by the NIH T32 EB001026
617 - Cellular Approaches to Tissue Engineering and Regeneration, Cardiovascular Bioengineering
618 Training Program T32-HL076124, and Ruth L. Kirschstein National Research Service Award

(NRSA) Individual Predoctoral Fellowship (Parent F31) 1F31AR083814 - 01A1. The authors thank the funding support from the NIH (P30AG038072). The Chicago Center on Musculoskeletal Pain Research Core Center, supported by NIH P30AR079206, provided training on pain-assessing methods. Schematic figures were created at https://BioRender.com.

Data Availability

The Raw and processed RNA-seq data was uploaded to Gene Expression Omnibus (GEO) with accession ID: GSE287861. The data will be publicly available when the manuscript is accepted.

627 **References**
628

629 1. Xiong, H., Hua, F., Dong, Y., Lin, Y., Ying, J., Liu, J., Wang, X., Zhang, L., and Zhang, J.
630 (2022). DNA damage response and GATA4 signaling in cellular senescence and aging-
631 related pathology. Front Aging Neurosci *14*, 933015. 10.3389/fnagi.2022.933015.
632 2. Rahmati, M., Nalesso, G., Mobasheri, A., and Mozafari, M. (2017). Aging and
633 osteoarthritis: Central role of the extracellular matrix. Ageing Res Rev *40*, 20-30.
634 10.1016/j.arr.2017.07.004.
635 3. Makarczyk, M.J., Gao, Q., He, Y., Li, Z., Gold, M.S., Hochberg, M.C., Bunnell, B.A.,
636 Tuan, R.S., Goodman, S.B., and Lin, H. (2021). Current Models for Development of
637 Disease-Modifying Osteoarthritis Drugs. Tissue Eng Part C Methods *27*, 124-138.
638 10.1089/ten.TEC.2020.0309.
639 4. Hawker, G.A., and King, L.K. (2022). The Burden of Osteoarthritis in Older Adults. Clin
640 Geriatr Med *38*, 181-192. 10.1016/j.cger.2021.11.005.
641 5. Copp, M.E., Chubinskaya, S., Bracey, D.N., Shine, J., Sessions, G., Loeser, R.F., and
642 Diekman, B.O. (2022). Comet assay for quantification of the increased DNA damage
643 burden in primary human chondrocytes with aging and osteoarthritis. Aging Cell *21*,
644 e13698. 10.1111/acel.13698.
645 6. Loeser, R.F., Collins, J.A., and Diekman, B.O. (2016). Ageing and the pathogenesis of
646 osteoarthritis. Nat Rev Rheumatol *12*, 412-420. 10.1038/nrrheum.2016.65.
647 7. Ji, M.L., Jiang, H., Li, Z., Geng, R., Hu, J.Z., Lin, Y.C., and Lu, J. (2022). Sirt6 attenuates
648 chondrocyte senescence and osteoarthritis progression. Nat Commun *13*, 7658.
649 10.1038/s41467-022-35424-w.
650 8. Franceschi, C., Bonafe, M., Valensin, S., Olivieri, F., De Luca, M., Ottaviani, E., and De
651 Benedictis, G. (2000). Inflamm-aging. An evolutionary perspective on
652 immunosenescence. Ann N Y Acad Sci *908*, 244-254. 10.1111/j.1749-
653 6632.2000.tb06651.x.
654 9. Makarczyk, M.J. (2023). Cell Therapy Approaches for Articular Cartilage Regeneration.
655 Organogenesis *19*, 2278235. 10.1080/15476278.2023.2278235.
656 10. Kang, C., Xu, Q., Martin, T.D., Li, M.Z., Demaria, M., Aron, L., Lu, T., Yankner, B.A.,
657 Campisi, J., and Elledge, S.J. (2015). The DNA damage response induces inflammation
658 and senescence by inhibiting autophagy of GATA4. Science *349*, aaa5612.
659 10.1126/science.aaa5612.
660 11. Kang, D., Shin, J., Cho, Y., Kim, H.S., Gu, Y.R., Kim, H., You, K.T., Chang, M.J., Chang,
661 C.B., Kang, S.B., et al. (2019). Stress-activated miR-204 governs senescent phenotypes
662 of chondrocytes to promote osteoarthritis development. Sci Transl Med *11*.
663 10.1126/scitranslmed.aar6659.
664 12. Li, Z., Lin, Z., Liu, S., Yagi, H., Zhang, X., Yocum, L., Romero-Lopez, M., Rhee, C.,
665 Makarcyzk, M.J., Yu, I., et al. (2022). Human Mesenchymal Stem Cell-Derived
666 Miniature Joint System for Disease Modeling and Drug Testing. Adv Sci (Weinh) *9*,
667 e2105909. 10.1002/advs.202105909.
668 13. Glasson, S.S., Blanchet, T.J., and Morris, E.A. (2007). The surgical destabilization of the
669 medial meniscus (DMM) model of osteoarthritis in the 129/SvEv mouse. Osteoarthritis
670 Cartilage *15*, 1061-1069. 10.1016/j.joca.2007.03.006.

14. Chen, D., Shen, J., Zhao, W., Wang, T., Han, L., Hamilton, J.L., and Im, H.J. (2017). Osteoarthritis: toward a comprehensive understanding of pathological mechanism. Bone Res *5*, 16044. 10.1038/boneres.2016.44.
15. Barton, N.J., Strickland, I.T., Bond, S.M., Brash, H.M., Bate, S.T., Wilson, A.W., Chessell, I.P., Reeve, A.J., and McQueen, D.S. (2007). Pressure application measurement (PAM): a novel behavioural technique for measuring hypersensitivity in a rat model of joint pain. J Neurosci Methods *163*, 67-75. 10.1016/j.jneumeth.2007.02.012.
16. Leuchtweis, J., Imhof, A.K., Montechiaro, F., Schaible, H.G., and Boettger, M.K. (2010). Validation of the digital pressure application measurement (PAM) device for detection of primary mechanical hyperalgesia in rat and mouse antigen-induced knee joint arthritis. Methods Find Exp Clin Pharmacol *32*, 575-583. 10.1358/mf.2010.32.8.1532102.
17. Hayer, S., Vervoordeldonk, M.J., Denis, M.C., Armaka, M., Hoffmann, M., Bäcklund, J., Nandakumar, K.S., Niederreiter, B., Geka, C., Fischer, A., et al. (2021). 'SMASH' recommendations for standardised microscopic arthritis scoring of histological sections from inflammatory arthritis animal models. Ann Rheum Dis *80*, 714-726. 10.1136/annrheumdis-2020-219247.
18. Wang, X.H., Gao, J.W., Bao, J.P., Zhu, L., Xie, Z.Y., Chen, L., Peng, X., Zhang, C., and Wu, X.T. (2022). GATA4 promotes the senescence of nucleus pulposus cells via NF-kappaB pathway. Arch Gerontol Geriatr *101*, 104676. 10.1016/j.archger.2022.104676.
19. Shi, W., Zheng, Y., Luo, S., Li, X., Zhang, Y., Meng, X., Huang, C., and Li, J. (2021). METTL3 Promotes Activation and Inflammation of FLSs Through the NF-kappaB Signaling Pathway in Rheumatoid Arthritis. Front Med (Lausanne) *8*, 607585. 10.3389/fmed.2021.607585.
20. Chen, X., Gong, W., Shao, X., Shi, T., Zhang, L., Dong, J., Shi, Y., Shen, S., Qin, J., Jiang, Q., and Guo, B. (2022). METTL3-mediated m(6)A modification of ATG7 regulates autophagy-GATA4 axis to promote cellular senescence and osteoarthritis progression. Ann Rheum Dis *81*, 87-99. 10.1136/annrheumdis-2021-221091.
21. Garcia de Vinuesa, A., Sanchez-Duffhues, G., Blaney-Davidson, E., van Caam, A., Lodder, K., Ramos, Y., Kloppenburg, M., Meulenbelt, I., van der Kraan, P., Goumans, M.J., and Ten Dijke, P. (2021). Cripto favors chondrocyte hypertrophy via TGF-beta SMAD1/5 signaling during development of osteoarthritis. J Pathol *255*, 330-342. 10.1002/path.5774.
22. Barbero, A., Grogan, S., Schafer, D., Heberer, M., Mainil-Varlet, P., and Martin, I. (2004). Age related changes in human articular chondrocyte yield, proliferation and post-expansion chondrogenic capacity. Osteoarthritis Cartilage *12*, 476-484. 10.1016/j.joca.2004.02.010.
23. Forsyth, C.B., Cole, A., Murphy, G., Bienias, J.L., Im, H.J., and Loeser, R.F., Jr. (2005). Increased matrix metalloproteinase-13 production with aging by human articular chondrocytes in response to catabolic stimuli. J Gerontol A Biol Sci Med Sci *60*, 1118-1124. 10.1093/gerona/60.9.1118.
24. van der Kraan, P.M. (2017). The changing role of TGFbeta in healthy, ageing and osteoarthritic joints. Nat Rev Rheumatol *13*, 155-163. 10.1038/nrrheum.2016.219.
25. Shen, H., He, Y., Wang, N., Fritch, M.R., Li, X., Lin, H., and Tuan, R.S. (2021). Enhancing the potential of aged human articular chondrocytes for high-quality cartilage regeneration. FASEB J *35*, e21410. 10.1096/fj.202002386R.

716 26. Romano, O., and Miccio, A. (2020). GATA factor transcriptional activity: Insights from
717 genome-wide binding profiles. IUBMB Life *72*, 10-26. 10.1002/iub.2169.
718 27. Dobrzycki, T., Lalwani, M., Telfer, C., Monteiro, R., and Patient, R. (2020). The roles
719 and controls of GATA factors in blood and cardiac development. IUBMB Life *72*, 39-44.
720 10.1002/iub.2178.
721 28. Ang, Y.S., Rivas, R.N., Ribeiro, A.J.S., Srivas, R., Rivera, J., Stone, N.R., Pratt, K.,
722 Mohamed, T.M.A., Fu, J.D., Spencer, C.I., et al. (2016). Disease Model of GATA4
723 Mutation Reveals Transcription Factor Cooperativity in Human Cardiogenesis. Cell *167*,
724 1734-1749 e1722. 10.1016/j.cell.2016.11.033.
725 29. Villamayor, L., Cano, D.A., and Rojas, A. (2020). GATA factors in pancreas development
726 and disease. IUBMB Life *72*, 80-88. 10.1002/iub.2170.
727 30. Tremblay, M., Sanchez-Ferras, O., and Bouchard, M. (2018). GATA transcription factors
728 in development and disease. Development *145*. 10.1242/dev.164384.
729 31. Molkentin, J.D. (2000). The zinc finger-containing transcription factors GATA-4, -5, and
730 -6. Ubiquitously expressed regulators of tissue-specific gene expression. J Biol Chem
731 *275*, 38949-38952. 10.1074/jbc.R000029200.
732 32. Jiao, H., Walczak, B.E., Lee, M.S., Lemieux, M.E., and Li, W.J. (2021). GATA6 regulates
733 aging of human mesenchymal stem/stromal cells. Stem Cells *39*, 62-77.
734 10.1002/stem.3297.
735 33. Mahmoud, M., Souilhol, C., Serbanovic-Canic, J., and Evans, P. (2019). GATA4-Twist1
736 Signalling in Disturbed Flow-Induced Atherosclerosis. Cardiovasc Drugs Ther *33*, 231-
737 237. 10.1007/s10557-019-06863-3.
738 34. Katanasaka, Y., Suzuki, H., Sunagawa, Y., Hasegawa, K., and Morimoto, T. (2016).
739 Regulation of Cardiac Transcription Factor GATA4 by Post-Translational Modification in
740 Cardiomyocyte Hypertrophy and Heart Failure. Int Heart J *57*, 672-675. 10.1536/ihj.16-
741 404.
742 35. Chung, Y.P., Weng, T.I., Chan, D.C., Yang, R.S., and Liu, S.H. (2023). Low-dose
743 tributyltin triggers human chondrocyte senescence and mouse articular cartilage aging.
744 Arch Toxicol *97*, 547-559. 10.1007/s00204-022-03407-x.
745 36. Chung, Y.P., Chen, Y.W., Weng, T.I., Yang, R.S., and Liu, S.H. (2020). Arsenic induces
746 human chondrocyte senescence and accelerates rat articular cartilage aging. Arch Toxicol
747 *94*, 89-101. 10.1007/s00204-019-02607-2.
748 37. Thielen, N.G.M., van Caam, A.P.M., HM, V.B., Vitters, E.L., van den Bosch, M.H.J.,
749 Koenders, M.I., van de Loo, F.A.J., Blaney Davidson, E.N., and van der Kraan, P.M.
750 (2023). Separating friend from foe: Inhibition of TGF-beta-induced detrimental
751 SMAD1/5/9 phosphorylation while maintaining protective SMAD2/3 signaling in OA
752 chondrocytes. Osteoarthritis Cartilage *31*, 1481-1490. 10.1016/j.joca.2023.08.004.
753 38. van der Kraan, P.M., Goumans, M.J., Blaney Davidson, E., and ten Dijke, P. (2012). Age-
754 dependent alteration of TGF-beta signalling in osteoarthritis. Cell Tissue Res *347*, 257-
755 265. 10.1007/s00441-011-1194-6.
756 39. Bauge, C., Girard, N., Lhuissier, E., Bazille, C., and Boumediene, K. (2014). Regulation
757 and Role of TGFbeta Signaling Pathway in Aging and Osteoarthritis Joints. Aging Dis *5*,
758 394-405. 10.14336/AD.2014.0500394.
759 40. van Caam, A., Madej, W., Garcia de Vinuesa, A., Goumans, M.J., Ten Dijke, P., Blaney
760 Davidson, E., and van der Kraan, P. (2017). TGFbeta1-induced SMAD2/3 and SMAD1/5

761 phosphorylation are both ALK5-kinase-dependent in primary chondrocytes and mediated
762 by TAK1 kinase activity. Arthritis Res Ther *19*, 112. 10.1186/s13075-017-1302-4.
763 41. Wiegertjes, R., Thielen, N.G.M., van Caam, A.P.M., van Laar, M., van Beuningen, H.M.,
764 Koenders, M.I., van Lent, P., van der Kraan, P.M., van de Loo, F.A.J., and Blaney
765 Davidson, E.N. (2021). Increased IL-6 receptor expression and signaling in ageing
766 cartilage can be explained by loss of TGF-beta-mediated IL-6 receptor suppression.
767 Osteoarthritis Cartilage *29*, 773-782. 10.1016/j.joca.2021.01.008.
768 42. Lee, G.T., Kwon, S.J., Lee, J.H., Jeon, S.S., Jang, K.T., Choi, H.Y., Lee, H.M., Kim, W.J.,
769 Kim, S.J., and Kim, I.Y. (2010). Induction of interleukin-6 expression by bone
770 morphogenetic protein-6 in macrophages requires both SMAD and p38 signaling
771 pathways. J Biol Chem *285*, 39401-39408. 10.1074/jbc.M110.103705.
772 43. Yao, Q., Wu, X., Tao, C., Gong, W., Chen, M., Qu, M., Zhong, Y., He, T., Chen, S., and
773 Xiao, G. (2023). Osteoarthritis: pathogenic signaling pathways and therapeutic targets.
774 Signal Transduct Target Ther *8*, 56. 10.1038/s41392-023-01330-w.
775 44. Adler, A.S., Sinha, S., Kawahara, T.L., Zhang, J.Y., Segal, E., and Chang, H.Y. (2007).
776 Motif module map reveals enforcement of aging by continual NF-kappaB activity. Genes
777 Dev *21*, 3244-3257. 10.1101/gad.1588507.
778 45. Rahman, S.M.T., Aqdas, M., Martin, E.W., Tomassoni Ardori, F., Songkiatisak, P., Oh,
779 K.S., Uderhardt, S., Yun, S., Claybourne, Q.C., McDevitt, R.A., et al. (2022). Double
780 knockin mice show NF-kappaB trajectories in immune signaling and aging. Cell Rep *41*,
781 111682. 10.1016/j.celrep.2022.111682.
782 46. Qiao, W., Huang, Y., Bian, Z., Sun, X., Wang, X., Gao, Q., Peng, Y., and Meng, L.
783 (2019). Lipopolysaccharide-induced DNA damage response activates nuclear factor
784 kappaB signalling pathway via GATA4 in dental pulp cells. Int Endod J *52*, 1704-1715.
785 10.1111/iej.13180.
786 47. Jia, W., Wu, W., Yang, D., Xiao, C., Huang, M., Long, F., Su, Z., Qin, M., Liu, X., and
787 Zhu, Y.Z. (2018). GATA4 regulates angiogenesis and persistence of inflammation in
788 rheumatoid arthritis. Cell Death Dis *9*, 503. 10.1038/s41419-018-0570-5.
789 48. Marechal, A., and Zou, L. (2013). DNA damage sensing by the ATM and ATR kinases.
790 Cold Spring Harb Perspect Biol *5*. 10.1101/cshperspect.a012716.
791 49. Menolfi, D., and Zha, S. (2020). ATM, ATR and DNA-PKcs kinases-the lessons from the
792 mouse models: inhibition not equal deletion. Cell Biosci *10*, 8. 10.1186/s13578-020-
793 0376-x.
794 50. Wang, Y., Zhang, N., Zhang, L., Li, R., Fu, W., Ma, K., Li, X., Wang, L., Wang, J.,
795 Zhang, H., et al. (2016). Autophagy Regulates Chromatin Ubiquitination in DNA
796 Damage Response through Elimination of SQSTM1/p62. Mol Cell *63*, 34-48.
797 10.1016/j.molcel.2016.05.027.
798

799

800

801

802

803

Supplementary Figures and Tables

Figure S1

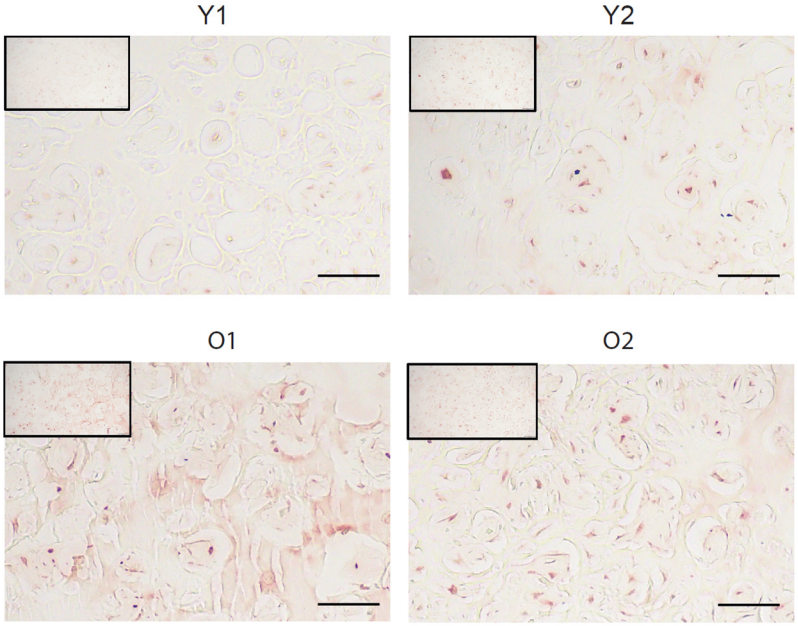

Figure S1. *GATA4 IHC of healthy human cartilage tissue from 3 young (Y1,Y2) and aged (O1,O2) donors. Scale Bar=50 µm.*

Figure S2

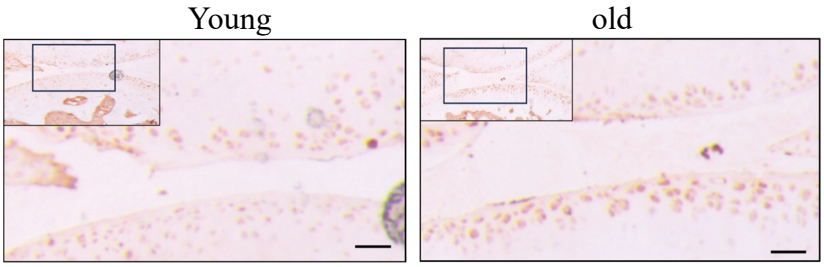

Figure S2. *GATA4 IHC of healthy mouse cartilage tissue from young (left) and old (right) mice. Scale Bar=50 µm.*

826 **Figure S3**

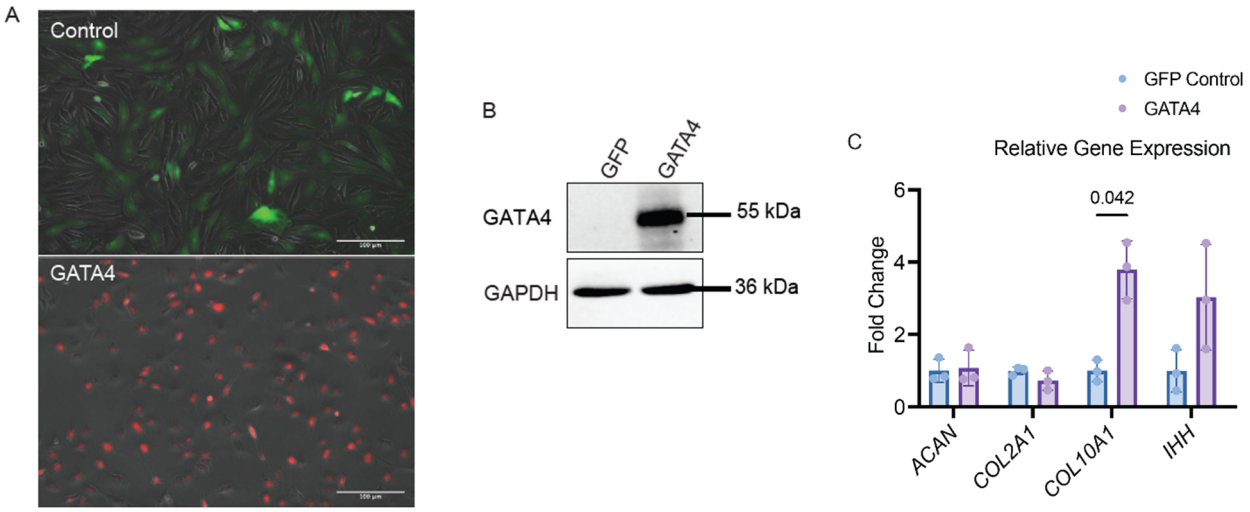

827
828 ***Figure S3.*** *(A) GATA4 overexpression of young, pooled chondrocytes in monolayer culture 48*
829 *hours after infection. The lentiviral control contained the EF1A promoter-driven expression of*
830 *Green Fluorescent Protein (GFP), and the GATA4 lentivirus contained the EF1A promoter-driven*
831 *overexpression of GATA4 with dTomato fluorescent protein. Scale Bar=100 µm. (B) Western blot*
832 *to measure GATA4 protein levels. (C) RT-qPCR analysis of relative gene expression of cartilage*
833 *matrix proteins aggrecan (ACAN) and collagen type II-α1 (COL2A1), and hypertrophy markers*
834 *collagen type X- α1 (COL10A1) and India hedgehog (IHH).*
835
836
837
838
839
840
841
842
843
844
845
846
847
848
849
850
851
852
853
854
855
856
857
858

859 **Figure S4**

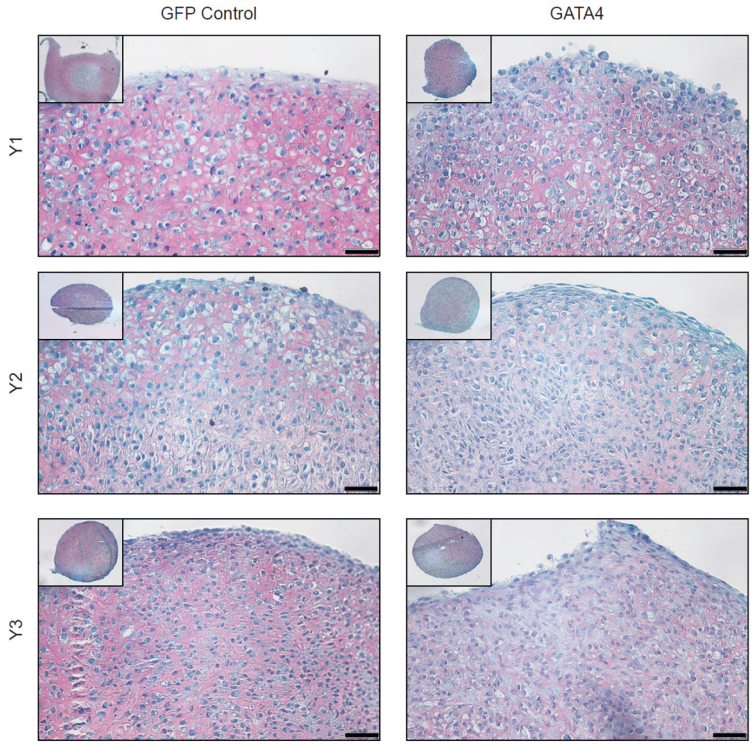

860

861 ***Figure S4.*** *Safranin-O staining for pellets derived from young, individual chondrocyte (Y1-3)*
862 *transduced with GFP control lentivirus or GATA4 lentivirus. Pellets were cultured in chondrogenic*
863 *medium for 7 days. Scale Bar=50 μm.*
864
865
866
867
868
869 ***Figure S5***
870

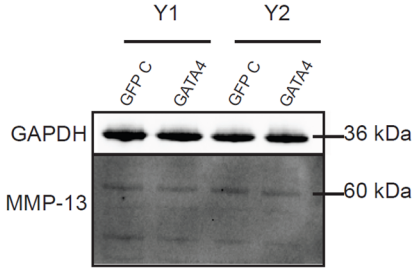

871
872
873 ***Figure S5.*** *Western blot to examine MMP-13 protein levels in pellets derived from two young*
874 *chondrocyte lines (Y1 and Y2) overexpressing GFP control (GFP C) or GATA4.*
875
876
877
878

879 ***Figure S6***

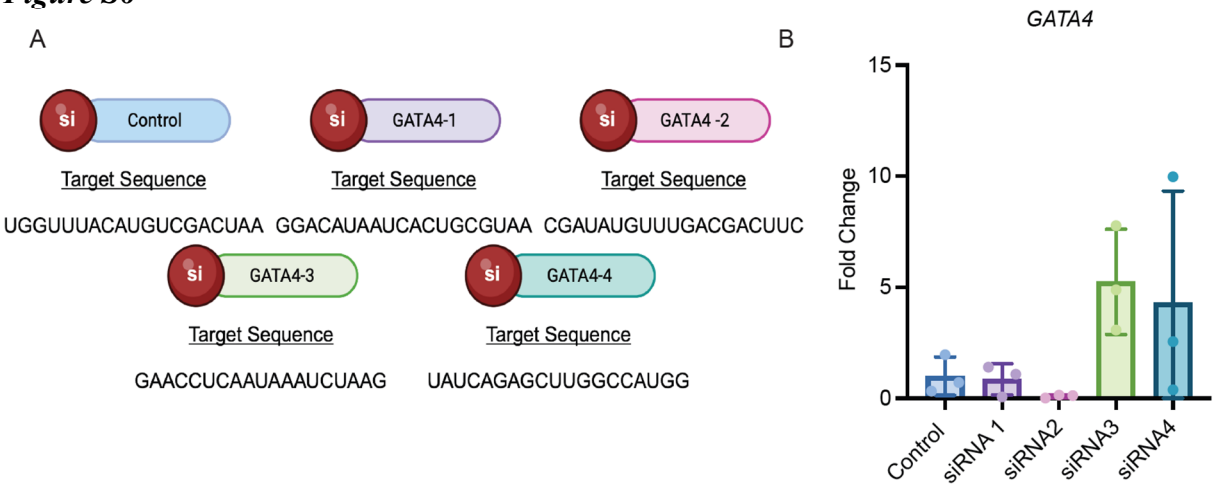

880
881 ***Supplementary Figure 6. Assessment of GATA4 siRNAs in monolayer***. *(A) Schematic of the four*
882 *different GATA4 siRNAs with corresponding target sequences assessed for GATA4 knockdown in*
883 *monolayer culture of old pooled chondrocytes. (B) RT-qPCR assessing GATA4 levels after siRNA*
884 *treatment (n=3).*
885
886
887
888 **Figure S7**

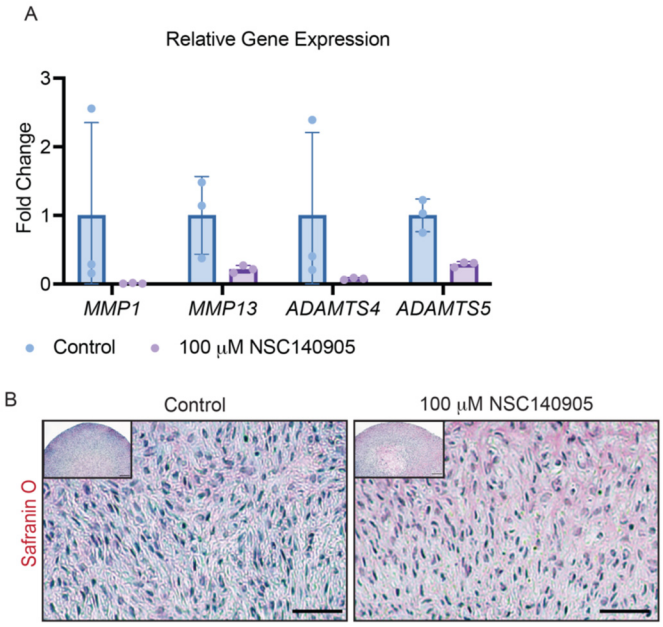

889
890 ***Supplementary Figure 7. Assessment of GATA4 small molecule inhibitor, NSC140905.*** *Pooled*
891 *old human chondrocytes were pelleted and treated with the chondrogenic medium with or without*
892 *supplanting NSC140905 for 14 days. (A) RT-qPCR analysis of relative gene expression of matrix-*
893 *degrading enzymes, including MMP-1,13 and ADAMTS 4 and 5 (n=3). Student's two-tailed t-test*
894 *with Welch's correction for standard deviation and a p-value of 0.05 was used for all statistical*
895 *analysis. (B) Safranin-O/Fast green staining. Bar=50 μM.*
896

Figure S8

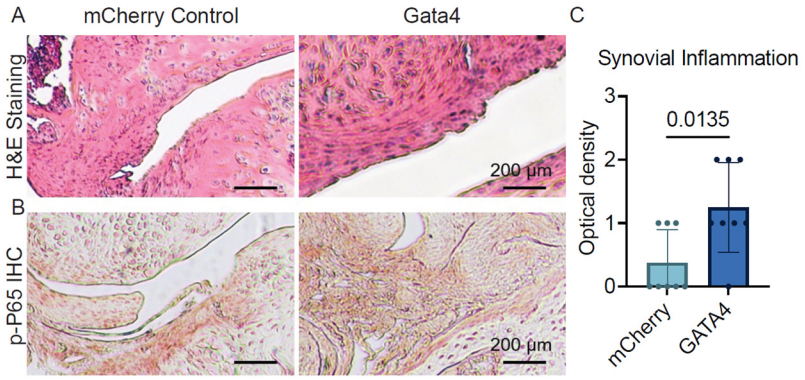

Supplementary Figure S8. *(A) H&E staining and (B) p-P65 IHC to assess synovial inflammation in mice treated with lentiviral vectors carrying mCherry Control or Gata4.* C. p-P65 IHC staining was also semi-quantitated.

Figure S9

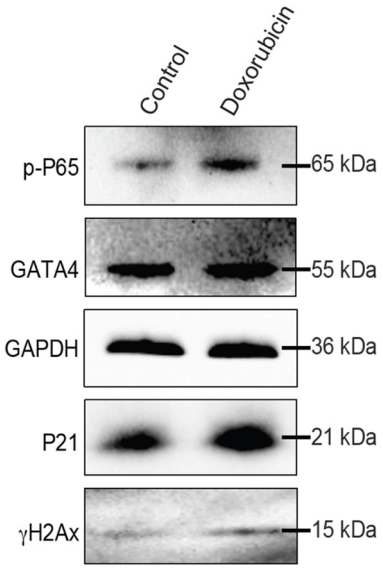

Supplementary Figure S9. *Wester blot to examine protein levels in chondrocytes treated with doxorubicin (100nM) or vehicle control for 3 days.*

919 **Table S1. Information of chondrocyte donors**

920 RNA sequencing

Age	Gender
24	Female
36	Female
38	Female
70	Female
73	Female
74	Female

921

922 Western Blot

Age	Gender
22	Male
26	Male
29	Male
69	Male
70	Male
73	Female

923

924

925 Human Cartilage Tissue IHC

Age	Gender
24	Male
25	Female
27	Female
33	Male
67	Female
76	Female
78-1	Female
78-2	Male

926

927 Young Chondrocyte Pool

Age	Gender
22	Male
29	Male
38	Female
42	Female

928

929 Old Chondrocyte Pool #1

Age	Gender
66	Male
70	Male
73	Female

930

931 Old Chondrocyte Pool #2

Age	Gender
66-1	Male
66-2	Male
70-1	Male
70-2	Male

Monolayer young individual chondrocytes

Age	Gender
29	Male
36	Female
38	Female

Pellet young individual chondrocytes

Age	Gender
21	Male
35	Male
38	Female

938 **Table S2. Antibodies used for immunofluorescence (IF), Immunohistochemistry (IHC), or**
939 **Western blot (WB)**

Antibody	Origin	Cat. No	Species	Assay	Dilution
Anti-Human Collagen Type II	MP Biomedicals	SKU 0863171	Mouse	IHC	1:200
Biotinylated Goat Anti-Rabbit IgG	Vector Laboratories	PK-6101	Rabbit	IHC	1:50
Goat Anti-Rabbit IgG H&L (HRP)	Abcam	Ab6721	Goat	WB	1:5000
GAPDH (D16H11) XP® Rabbit mAb	Cell Signaling Technology	5174s	Rabbit	WB	1:2000
Smad1 (D59D7) XP® Rabbit mAb	Cell Signaling Technology	6944s	Rabbit	WB	1:500
Anti-GATA4 antibody (ab84593)- Discontinued	Abcam	ab84593	Rabbit	IHC/WB	1:500
GATA-4 (D3A3M) Rabbit mAb	Cell Signaling Technology	369366s	Rabbit	IHC/WB	1:1000
Phospho-Smad1/5 (Ser463/465) (41D10) Rabbit mAb	Cell Signaling Technology	9516s	Rabbit	WB	1:500
Phospho-Smad2 (Ser465/467) (138D4) Rabbit mAb	Cell Signaling Technology	3108s	Rabbit	WB	1:500
Smad2/3 (D7G7) XP® Rabbit mAb	Cell Signaling Technology	8685s	Rabbit	WB	1:500
Anti-NF-kB p65 (phospho S536) antibody [EP2294Y]	Abcam	ab76302	Rabbit	WB	1:500
Anti-NF-kB p65 antibody [E379]	Abcam	ab32536	Rabbit	WB	1:500
Anti-p21 antibody [EPR362] - BSA and Azide free	Abcam	ab218311	Rabbit	WB	1:1000
Phospho-Histone H2A.X (Ser139) (20E3) Rabbit mAb	Cell Signaling Technology	9718s	Rabbit	WB	1:500

940
941
942
943
944
945

946 **Table S3: Full names of genes shown in Figure 1**

Transcription Regulator Name	Acronym
Hypoxia-inducible factor 1-alpha	HIF1A
GATA binding protein 4	GATA4
MAF bZIP transcription factor B	MAFB
Homeobox D10	HOXD10
CCAAT enhancer binding protein alpha	CEBPA
Forkhead box L2	FOXL2
Caudal type homeobox 2	CDX2
Early Growth Response 1	EGR1
Signal Transducer and Activator of Transcription 3	STAT3
Paired Box 1	PAX1
Sequestosome 1	SQSTM1
Myocardin Related Transcription Factor B	MRTFB
WW Domain Binding Protein 2	WBP2
Scleraxis bHLH Transcription Factor	SCX
Twist Family bHLH Transcription Factor 1	TWIST1
Myocyte Enhancer Factor 2D	MEF2D
Lysine Methyltransferase 2D	KMT2D
Achaete-scute Family bHLH Transcription Factor 1	ASCL1
Recombination Signal Binding Protein for Immunoglobulin kappa J region	RBPJ
SIX homeobox 1	SIX1
FERM domain containing 3	FRMPD3
Ceruloplasmin	CP
SPARC related modular calcium binding 2	SMOC2
ATP binding cassette subfamily A member 13	ABCA13
Inositol 1,4,5-triphosphate receptor type 1	ITPR1
NIM1 serine/threonine protein kinase	NIM1K
Fibroblast growth factor 13	FGF13
Ankyrin repeat domain 12	ANKRD12
GTP binding protein overexpressed in skeletal muscle	GEM
erythroferrone	FAM132B
Pappalysin 1	PAPPA
PPARG coactivator 1 alpha	PPARGC1A
Synaptotagmin like 2	SYTL2
Leucine rich repeat transmembrane neuronal 2	LRRTM2
G protein-coupled receptor class C group 5 member B	GPRC5B
Polypeptide N-acetylgalactosaminyltransferase 15	GALNT15

Growth associated protein 43	GAP43
Fibroblast growth factor binding protein 1	FGFBP1
ATRX chromatin remodeler	ATRX
Protocadherin gamma subfamily B, 2	PCDHGB2
Calsyntenin 2	CLSTN2
Fibroblast growth factor binding protein 2	FGFBP2
Desmocollin 2	DSC2
TNF receptor superfamily member 21	TNFRSF21
Kinesin family member 13B	KIF13B
Plexin A2	PLXNA2
Cysteine rich protein 2	CRIP2
Cysteine rich protein 1	CRIP1
KLF transcription factor 2	KLF2
Serum/glucocorticoid regulated kinase 1	SGK1
LIM zinc finger domain containing 2	LIMS2
Long intergenic non-protein coding RNA 1133	LINC01133
Adipogenesis regulatory factor	ADIRF
Ornithine decarboxylase 1	ODC1
Kazrin, periplakin interacting protein	KAZN
Chondroitin polymerizing factor	CHPF
RAB23, member RAS oncogene family	RAB23
Alkaline phosphatase, biomineralization associated	ALPL
Signal transducer and activator of transcription 4	STAT4
G protein-coupled receptor 1	GPR1
Spectrin alpha, non-erythrocytic 1	SPTAN1
Very low density lipoprotein receptor	VLDLR
Fatty acid desaturase 3	FADS3
Cancer susceptibility candidate 4	CASC4
NAD(P)H quinone dehydrogenase 1	NQO1
Pyrroline-5-carboxylate reductase 1	PYCR1
ERBB receptor feedback inhibitor 1	ERRFI1
NmrA-like family domain containing 1 pseudogene	LOC344887
Desumoylating isopeptidase 2	DESI2
Basonuclin zinc finger protein 1	BNC1

947

948

949 **Table S4. Primers for qRT-PCR**

Gene	Forward primer (5'-3')	Reverse primer (5'-3')
RPL13A	GCCATCGTGGCTAAACAGGTA	GTTGGTGTTCATCCGCTTGC
GATA4	CAGTCTACGTGCCCACACC	TCCCGCCTGGCTCCAT
ACAN	AGTCACACCTGAGCAGCATC	AGTTCTCAAATTGCATGGGGTGTC
COL2A1	GGATGGCTGCACGAAACATACCGG	CAAGAAGCAGACCGGCCCTATG
COL10A1	CCCTCTTGTTAGTGCCAACC	AGATTCCAGTCCTTGGGTCA
IHH	AACTCGCTGGCTATCTCGGT	GCCCTCATAATGCAGGGACT
IL-6	ACTCACCTCTTCAGAACGAATTG	CCATCTTTGGAAGGTTCAGGTTG
IL-8	TTTTGCCAAGGAGTGCTAAAGA	AACCCTCTGCACCCAGTTTTC
TNF-α	CCTCTCTCTAATCAGCCCTCTG	GAGGACCTGGGAGTAGATGAG
MMP-1	AAAATTACACGCCAGATTTGCC	GGTGTGACATTACTCCAGAGTTG
MMP-2	GGTCACATCGCTCCAGACT	TACAGGATCATTGGCTACACACC
MMP-3	CGGTTCCGCCTGTCTCAAG	CGCCAAAAGTGCCTGTCTT
MMP-12	GGAATCCTAGCCCATGCTTTT	CATTACGGCCTTTGGATCACT
MMP-13	ACTGAGAGGCTCCGAGAAATG	GAACCCCGCATCTTGGCTT
ADAMTS4	GAGGAGGAGATCGTGTTTCCA	CCAGCTCTAGTAGCAGCGTC
ADAMTS5	GAACATCGACCAACTCTACTCCG	CAATGCCCACCGAACCATCT

950

951

952

953 **Table S5. Information of Luminex assay kit**

Target Molecule	Method	Catalog number & supplier
IL-8	Luminex® assay	HAGP1MAG-12K, EMD Millipore
IL-6, CCL2, MMP-1, MMP-2, MMP-13.	Luminex® assay	LXSAHM-18, R&D Systems

954

955

956

957

958